RECORD
1997/7

GOVERNMENT OF
WESTERN AUSTRALIA

# ARCHAEAN GEOLOGY AND MINERALIZATION OF THE NORTHERN PART OF THE EASTERN GOLDFIELDS PROVINCE YILGARN CRATON, WESTERN AUSTRALIA — A FIELD GUIDE KALGOORLIE '97

compiled by S. Wyche

GEOLOGICAL SURVEY OF WESTERN AUSTRALIA

DEPARTMENT OF MINERALS AND ENERGY

GEOLOGICAL SURVEY OF WESTERN AUSTRALIA

Record 1997/7

# ARCHAEAN GEOLOGY AND MINERALIZATION OF THE NORTHERN PART OF THE EASTERN GOLDFIELDS PROVINCE, YILGARN CRATON, WESTERN AUSTRALIA — A FIELD GUIDE

## KALGOORLIE '97

compiled by
S. Wyche

contributions by
T. R. Farrell, S. Wyche, S. F. Liu[1], J. Landmark[2], M. Fletcher[3], and S. Hopf[3]

[1] Australian Geological Survey Organisation
[2] Great Central Mines NL, Bronzewing Operations
[3] WMC Resources Ltd, Mount Keith Operations

Perth 1997

MINISTER FOR MINES
The Hon. Norman Moore, MLC

ACTING DIRECTOR GENERAL
L. C. Ranford

DIRECTOR, GEOLOGICAL SURVEY OF WESTERN AUSTRALIA
Pietro Guj

National Library of Australia Card Number and ISBN 0 7309 6571 6

Copies available from:

Mining Information Centre
Department of Minerals and Energy
100 Plain Street
EAST PERTH, WESTERN AUSTRALIA 6004
Telephone: (08) 9222 3459 Fax: (08) 9222 3444

# Contents

# Figures

# Archaean geology and mineralization of the northern part of the Eastern Goldfields Province, Yilgarn Craton, Western Australia

# — a field guide

# Kalgoorlie '97

**Compiled by**
**S. Wyche**

**Contributors**
**T. R. Farrell, S. Wyche, S. F. Liu[1], J. Landmark[2]; M. Fletcher[3], and S. Hopf[3]**

## Introduction

**by S. Wyche, T. R. Farrell, and S. F. Liu**

This excursion guide examines the regional stratigraphy, deformation history and mineralization of late Archaean greenstones in the northern part of the Eastern Goldfields Province. Information in the guide was largely obtained in the course of regional mapping at 1:100 000 scale for the Eastern Goldfields program of the Geological Survey of Western Australia (GSWA)–Australian Geological Survey Organisation (AGSO) National Geoscience Mapping Accord (NGMA); specific information provided by mining companies is also included. The excursion traverses the major greenstone belts on SIR SAMUEL[4] and DUKETON (1:250 000), including sequences within the Agnew–Wiluna greenstone belt in the west, and the Yandal, Dingo Range, and Duketon greenstone belts farther east (Fig. 1).

The Eastern Goldfields Province (Griffin, 1990) is a major subdivision of the Archaean Yilgarn Craton (Myers, 1995). Its western boundary is marked by the Ida Fault, an easterly dipping craton-scale structure (Swager et al., 1997), and the eastern margin is concealed beneath Phanerozoic sedimentary rocks of the Officer Basin. The Province includes large areas of granitoid

---

1 Australian Geological Survey Organisation (AGSO)
2 Great Central Mines NL, Bronzewing Operations
3 WMC Resources Ltd, Mount Keith Operation
4 Capitalized names refer to standard map sheets

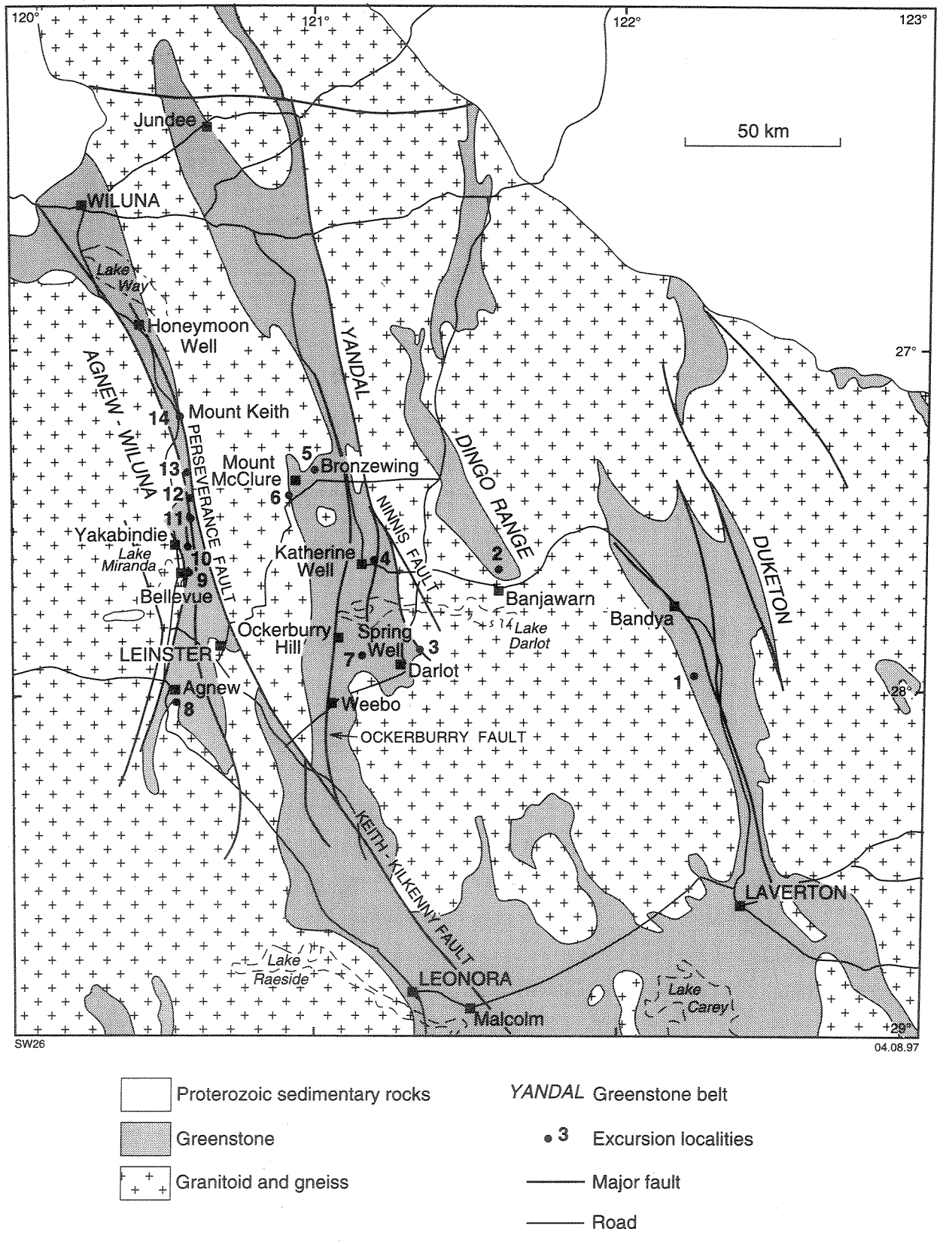


**Figure 1. Excursion localities, northern part of the Eastern Goldfields Province**

and gneiss with elongate, north to northwesterly trending 2.6–2.7 Ga greenstone belts. In contrast, limited Sensitive High-Resolution Ion Microprobe (SHRIMP) U–Pb zircon geochronological data (e.g. Wang et al., 1996) suggest that rocks of the Southern Cross Province to the west are dominantly c. 2.9–3.0 Ga old. However, zircon xenocrysts of similar age have been reported in a number of samples from the Eastern Goldfields Province (e.g. Compston et al., 1986; Nelson, 1995, 1996, 1997, in prep.). This suggests that the greenstone belts of the Eastern Goldfields Province were deposited on a sialic basement similar in age to the Southern Cross Province. The underlying sialic crust could have been the source for the enormous volumes of granitoid rock that were intruded during, and after, the main period of greenstone deposition.

Swager et al. (1995) and Swager (1995) divided the greenstones in the southern part of the Eastern Goldfields Province into tectonostratigraphic terranes bounded by major shear zones. Various schemes have been proposed to extend these terranes into the northern part of the Eastern Goldfields Province (Myers, 1995; Witt et al., 1996), but to date, there is no complete synthesis of the regional geology of this area.

Archaean greenstone belts in the northern part of the Eastern Goldfields Province contain similar rock sequences: however, there are significant differences in character between individual belts. The structural and metamorphic history is broadly similar to that described for greenstones to the south (Swager, 1997). All the greenstones are metamorphosed, as in other parts of the Eastern Goldfields Province, but primary features are commonly preserved, thus allowing the protoliths to be identified.

Four deformation events have been widely recognized in the northern part of the Eastern Goldfields Province. Little is known about the earliest deformation ($D_1$) because of overprinting by later structural and metamorphic events. It is not clear whether early fabrics ($D_1$) were produced by a thrusting event, like that identified in the Kalgoorlie–Kambalda area to the south (Swager et al., 1995). Additionally, the $D_1$ event in the Yakabindie area may not be the same as that described in the Duketon area. Significant shortening occurred during the second deformation event ($D_2$), resulting in tight folding and the formation of a strong regional foliation ($S_2$). However, the original orientation of $D_2$ structures is not clear because of reorientation during later deformation. The third deformation event is largely responsible for controlling the greenstone belt architecture. Regional-scale $D_3$ shear zones trend north-northwesterly, and are parallel to $F_3$ fold axes, the dominant foliation trends, and the strike of the greenstone belts. Late, crosscutting kink folds and crenulations in all greenstone belts are assigned to $D_4$. These deformation events have been numbered sequentially and may not be directly correlated with events recognized elsewhere in the Eastern Goldfields Province (cf. Hammond and Nisbet, 1992; Williams and Whitaker, 1993; Passchier, 1994; Swager et al., 1995; Swager, 1997). Late, easterly trending, regional-scale

structures that cut across all other structures (Fig. 1) may be related to early basin-forming events associated with the development of the Palaeoproterozoic Capricorn Orogen. These structures stand out on aeromagnetic and gravity maps, and they may separate blocks that have undergone differential uplift or subsidence.

All the greenstone sequences are metamorphosed, typically to greenschist facies, but areas that have undergone amphibolite facies metamorphism are common locally near granite–greenstone contacts. Peak metamorphism probably coincided with the emplacement of large monzogranite bodies during or after $D_2$. Amphibolite-facies assemblages defining $D_1$ fabrics in mafic and felsic gneisses also indicate that there was a significant metamorphic event during $D_1$. It is uncertain if this was a separate event, or whether it represents an early stage of a single metamorphic cycle.

Complex interleaving of granites and greenstones occurs along a number of granite–greenstone contacts, characterized by the local development of high-strain zones with shallow-plunging mineral lineations. Late granitoid intrusions, ranging in composition from syenite to diorite, cut across major structures, and therefore are probably younger than the regional $D_3$ shear zones. These bodies are particularly abundant in the Yandal greenstone belt. SHRIMP U–Pb zircon ages for granitoids range from 2738 ± 6 m.y. for a granitoid gneiss on the western side of the Yandal greenstone belt (Locality 6) to 2637 ± 8 m.y. for a monzogranite from between the Yandal and Duketon greenstone belts. A SHRIMP U–Pb zircon age of 2644 ± 13 m.y. for one of the quartz syenite bodies east of Bronzewing gold mine (AMG 51J 3241 69609)* is in the same range as ages obtained for similar bodies to the north in the Proterozoic Teague Ring structure on NABBERU (1:250 000), and to the south at McAuliffe Well on EDJUDINA (1:250 000; Nelson, 1997, in prep.).

The Agnew–Wiluna belt lies to the west of the Perseverance Fault, which is the northern extension of the Keith–Kilkenny lineament, or tectonic zone, of Hallberg (1985). This belt consists of metamorphosed ultramafic, mafic, felsic volcanic and sedimentary rocks. Ultramafic rocks in the belt are the host to four major nickel deposits, namely Perseverance (Leinster), Six Mile (Yakabindie), Mount Keith and Honeymoon Well (Fig. 1).

The Agnew–Wiluna belt is divided into two domains by the regionally extensive Jones Creek Conglomerate (Fig. 2). The western part of the belt, referred to as the Yakabindie greenstone sequence by Liu et al. (1997), comprises metamorphosed layered gabbro (Kathleen Valley Gabbro) and massive tholeiitic basalt (Mount Goode Basalt). The Kathleen Valley Gabbro dips moderately to steeply to the north-northwest, but compositional layering indicates that it is overturned. It consists predominantly of anorthositic gabbro in the north, gabbro in the hilly areas south of

---

* Grid references are specified using Australian Map Grid (AMG) coordinates in which the first set of characters refers to the map zone, and the subsequent sets of four figures (eastings) and five figures (northings) uniquely define the position to within 100 m.

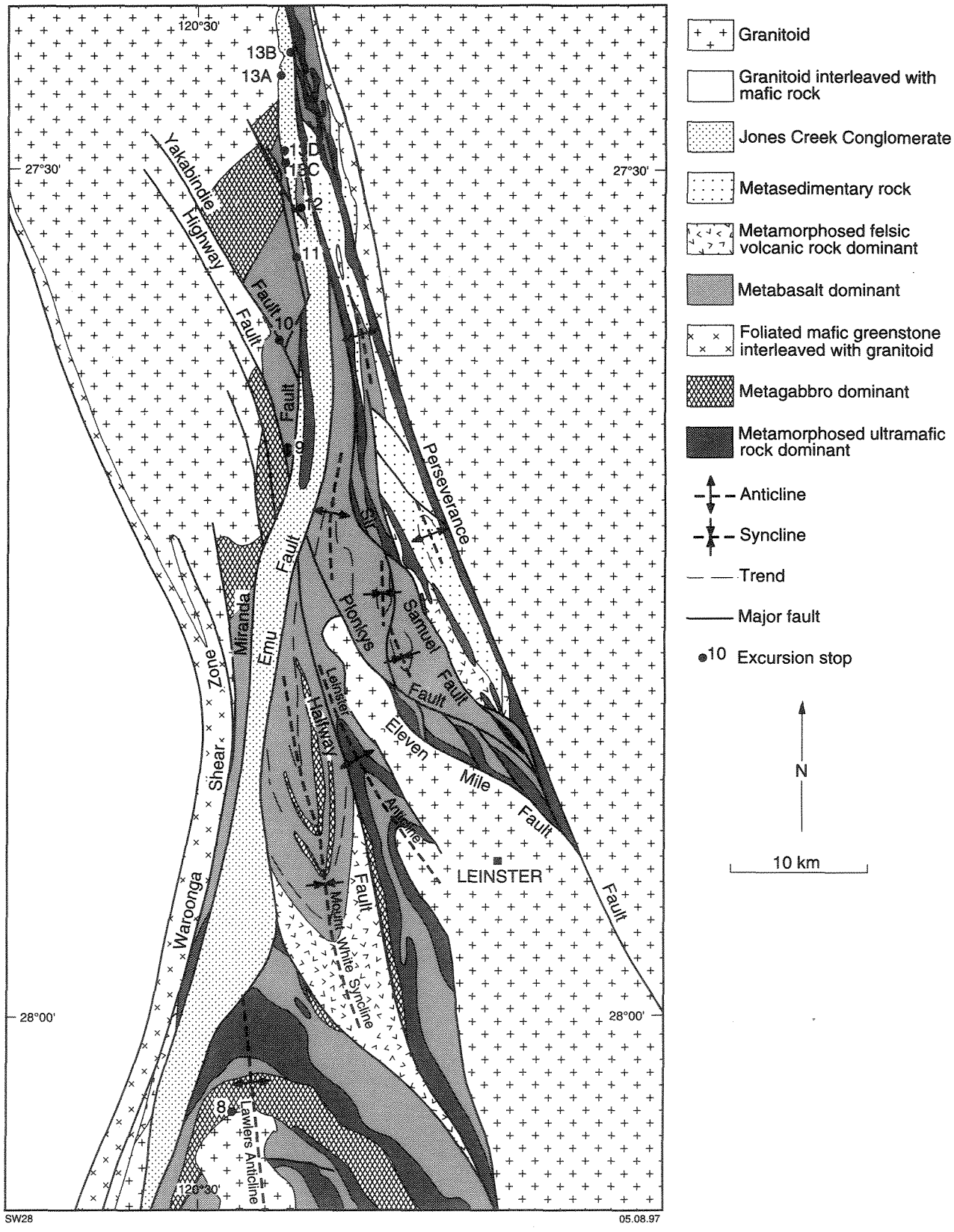


**Figure 2. Simplified geology of the southern part of the Agnew–Wiluna belt**

Kathleen Valley, and quartz-bearing gabbro to tonalite in the south, near the old Wiluna–Leinster road. The overlying Mount Goode Basalt consists of two units, with the upper unit containing locally abundant plagioclase phenocrysts and pillow structures.

The southern part of the Agnew–Wiluna belt, called the Agnew greenstone sequence by Liu et al. (1997), includes the Lawlers Anticline, the Mount White Syncline and the Leinster Anticline (Fig. 2). The western side of the belt is marked by the Jones Creek Conglomerate. The greenstone succession in the Lawlers Anticline includes metamorphosed ultramafic and felsic volcanic rocks, and metamorphosed basalt and gabbro. To the north, in the Mount White Syncline, the main rock type is metamorphosed basalt: metamorphosed gabbro and fine-grained sedimentary rock are subordinate. Greenstones between Plonkys Fault and Sir Samuel Fault are similar to those in the Mount White Syncline. Hill et al. (1995) interpreted the ultramafic rocks in this sequence as volcanic rocks that can be correlated along strike for more than 100 km. They were probably erupted during the same tectonomagmatic event that was responsible for the large volumes of komatiite in the southern part of the Eastern Goldfields Province.

The Yandal greenstone belt (Fig. 1) is divided into northern and southern sections separated by an attenuated zone north of the Bronzewing mine. This zone may represent a change in facies or a structural discontinuity between two sequences. The excursion visits localities in the southern section of the greenstone belt (Wyche and Westaway, 1995; Westaway and Wyche, in prep.).

The southern section of the Yandal belt is dominated by the calc-alkaline Spring Well felsic volcanic complex. A major structure, the Ockerburry Fault, trends north-northeast across the southern part of the Yandal greenstone belt. It is represented by a zone of strongly sheared rock, possibly more than 1 km wide (Fig. 1). West of the Ockerburry Fault there is a poorly exposed succession of felsic volcanic, volcaniclastic and sedimentary rocks. This sequence appears to overlie a better-exposed, east-younging sequence of mafic rocks that contains interbeds of chert, shale, tuffaceous sedimentary rocks and ultramafic units adjacent to the western greenstone contact. The area east of the Ockerburry Fault is dominated by the locally well-exposed Spring Well calc-alkaline volcanic complex (Giles, 1982; Westaway and Wyche, in prep.). Remnants of a probable subaerial volcanic centre are exposed near Spring Well. To the north and east, away from the volcanic centre, felsic tuffaceous and volcaniclastic rocks are interbedded with mafic volcanic rocks. There are numerous mafic intrusions throughout the sequence, many of which contain differentiation or layering.

The Dingo Range greenstone belt contains a metamorphosed mafic–ultramafic sequence with thin interbeds of metachert and strongly deformed metamorphosed felsic rock. The metamorphic grade reaches upper amphibolite facies in the southern part of the belt. The principal rock type in

this area is a fine- to medium-grained amphibolite. Thin units of tremolite–chlorite schist are abundant, and there are rare layers of talc–carbonate-altered komatiite.

The Duketon greenstone belt, which extends from the Duketon area south to Laverton, contains a wide range of rock types. They include metamorphosed chert, shale, sandstone, conglomerate, felsic volcanic and volcaniclastic rocks, as well as abundant metamorphosed mafic and ultramafic rocks. The central and northern parts of the belt are dominated by metamorphosed felsic volcanic and felsic sedimentary rock, including metamorphosed rhyolite and felsic tuff. Metamorphosed conglomerate with granitoid clasts that occurs close to the western margin of the greenstone belt may be equivalent to the Jones Creek Conglomerate.

Gold mineralization occurs in all the greenstone sequences. Gold has been deposited in a range of host rocks, where it is dominantly structurally controlled. It was probably deposited very late in the evolution of the granite–greenstone terrane. Economic nickel mineralization is confined to the thick ultramafic units in the Agnew–Wiluna belt.

# Excursion localities

## Locality 1: Murphy Hills — Duketon greenstone belt

### by T. R. Farrell

The Duketon greenstone belt encompasses a multiply deformed and metamorphosed, north-northwesterly trending sequence of Archaean supracrustal rocks, bordered by high-grade quartzofeldspathic gneiss and granitoids. The greenstone belt and the gneisses both show evidence of four phases of deformation (Farrell, 1995). Relationships between the greenstones, granitoids and gneisses are unclear, due largely to poor exposure of the contacts between rock units.

The purpose of the excursion stops in the Murphy Hills area (Fig. 3) is to examine the structural geology of the western margin of the Duketon greenstone belt, and to evaluate the nature of the 'granite–greenstone' contact. The excursion visits several critical outcrops, which show the overprinting of different generations of structures, to discuss implications for the tectonic interpretation of the Duketon greenstone belt. The Murphy Hills is a key location for studying granite–greenstone relationships because critical contacts are exposed in this area.

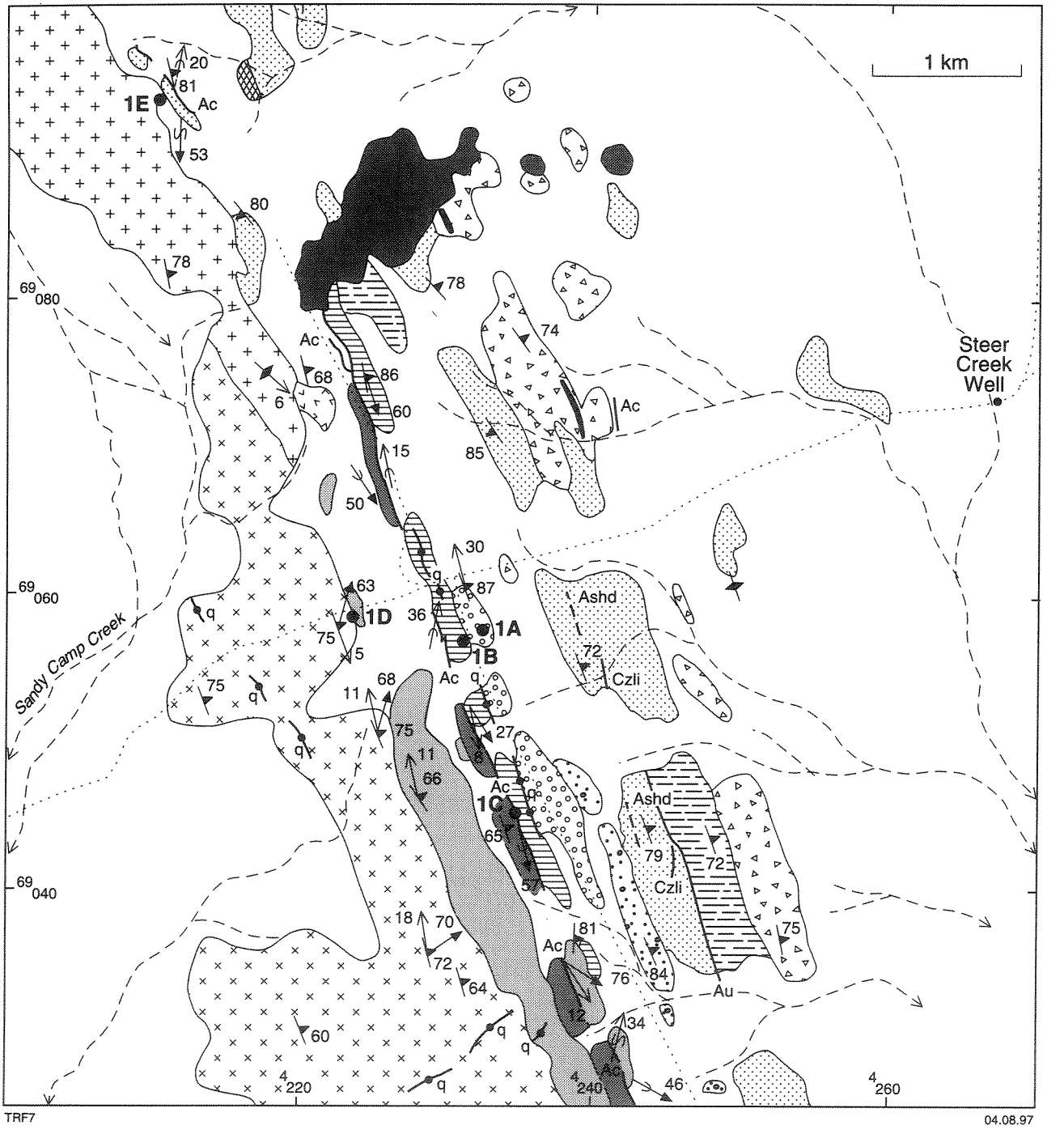


**Figure 3. Outcrop geology of the Murphy Hills area (legend on opposite page)**

The greenstone belt in the Murphy Hills area is metamorphosed to upper greenschist – lower amphibolite facies. The belt contains a sequence of amphibolite (with minor metagabbro), felsic schist, layered metachert, ultramafic schist, metaconglomerate and fine-grained metasedimentary rock. To the south, the greenstone belt is in contact with a zone of strongly deformed granitoid and quartzofeldspathic gneiss. By contrast, at the northern end of the Murphy Hills, the greenstones are

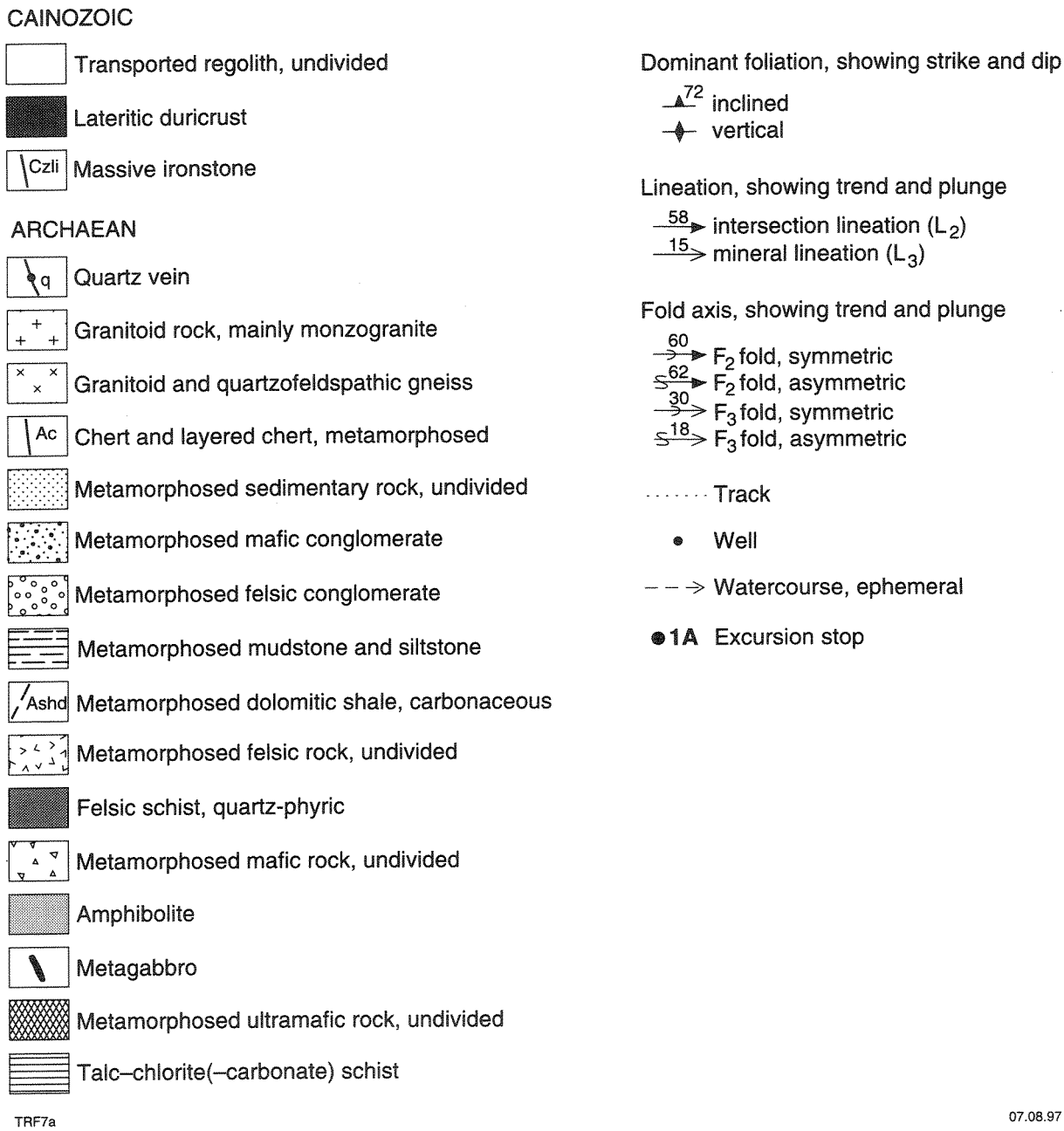


intruded by variably deformed granitoids. Three phases of deformation (correlated with $D_2$–$D_4$ of Farrell, 1995) are evident in rocks on both sides of the greenstone contact. An earlier deformation is inferred from structures present elsewhere in the Duketon area.

## Stop 1A: Deformed metaconglomerate — AMG 51J 4233 69058

A metamorphosed felsic conglomerate at this locality has many similarities to the Jones Creek Conglomerate in the Agnew–Wiluna belt (Durney, 1972; Marston and Travis, 1976; Liu et al., 1997). The metaconglomerate contains a range of clast types, including granitoid, quartz vein, felsic schist and rare ultramafic schist, ranging up to 150 mm in diameter. Granitoid clasts are dominant and the matrix is typically quartzofeldspathic (Fig. 4).

The metaconglomerate is strongly deformed and has a steeply dipping foliation and a moderate to shallow north-pitching mineral lineation. There is no evidence of earlier structures. The fabric is interpreted to have formed during $D_3$ because the mineral lineation is subparallel to $L_3$ mineral lineations elsewhere in the greenstone sequence and in deformed granitoids. Hence, the conglomerate was probably deposited after $D_2$ and before or early in $D_3$ — implying that there was uplift and erosion between $D_2$ and $D_3$. Some of the clasts have a sinistral asymmetry suggesting that $D_3$ may have involved a component of simple shear.

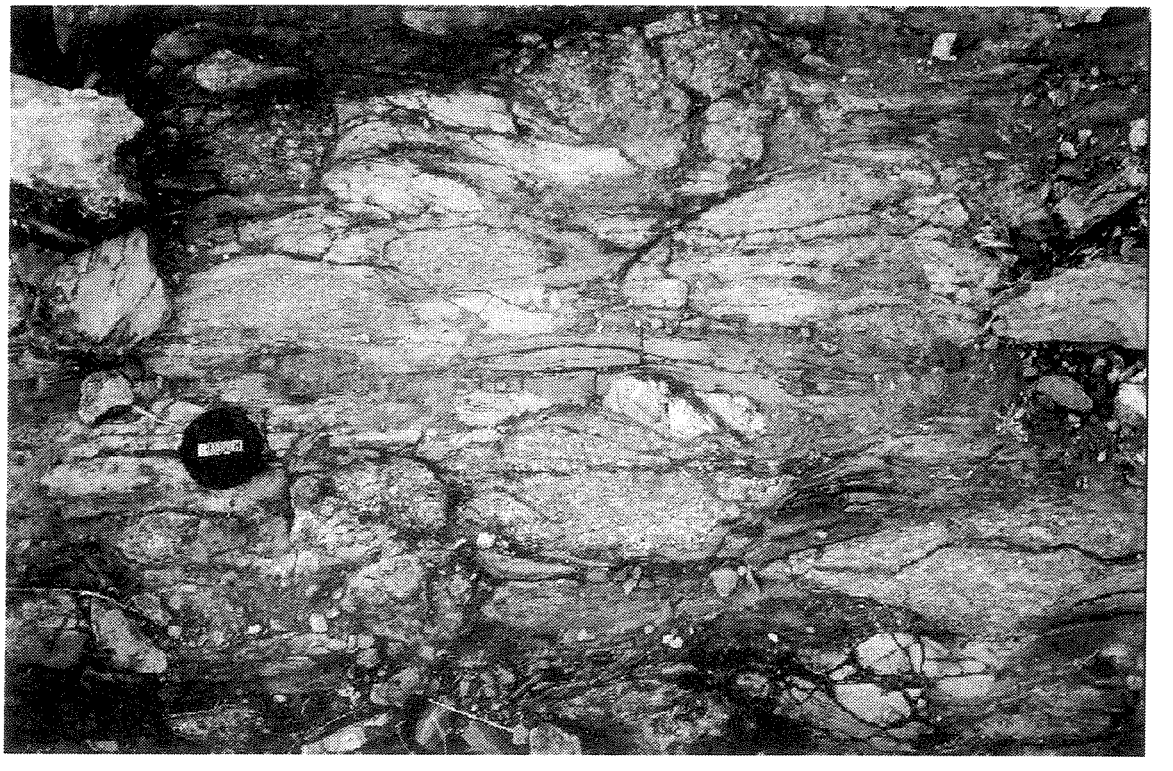

**Figure 4.** **Weathered exposure of strongly deformed, metamorphosed felsic conglomerate at Stop 1A. The conglomerate contains flattened clasts of fine- to medium-grained granitoid, vein quartz and ?felsic volcanic rocks. Note the distinct sinistral asymmetry of the clast of vein quartz**

## Stop 1B: Multiply deformed ultramafic schist — AMG 51J 4231 69056

Talc–chlorite schists at this location show evidence of two deformation events. They have a prominent, upright crenulation foliation ($S_3$), which overprints a tightly folded earlier fabric ($S_2$) and is parallel to the regional foliation (indicating that the regional foliation in many cases is probably a composite $S_2/S_3$ fabric). The fold axes ($F_3$) have a shallow plunge to the north and are approximately parallel to the mineral lineation in the rocks at Stop 1A.

## Stop 1C: Multiply deformed layered metachert — AMG 51J 4235 69045

Metamorphosed layered cherts along the western edge of the Duketon greenstone belt commonly show evidence of two penetrative deformation events. They contain a strong composite $S_0/S_2$ fabric containing rootless intrafolial $F_2$ folds (Fig. 5). The folds are typically upright, tight to isoclinal, have a similar geometry and a moderately steep plunge to the south. The fold axes are parallel to a prominent, combined intersection/mineral lineation defined mainly by the intersection

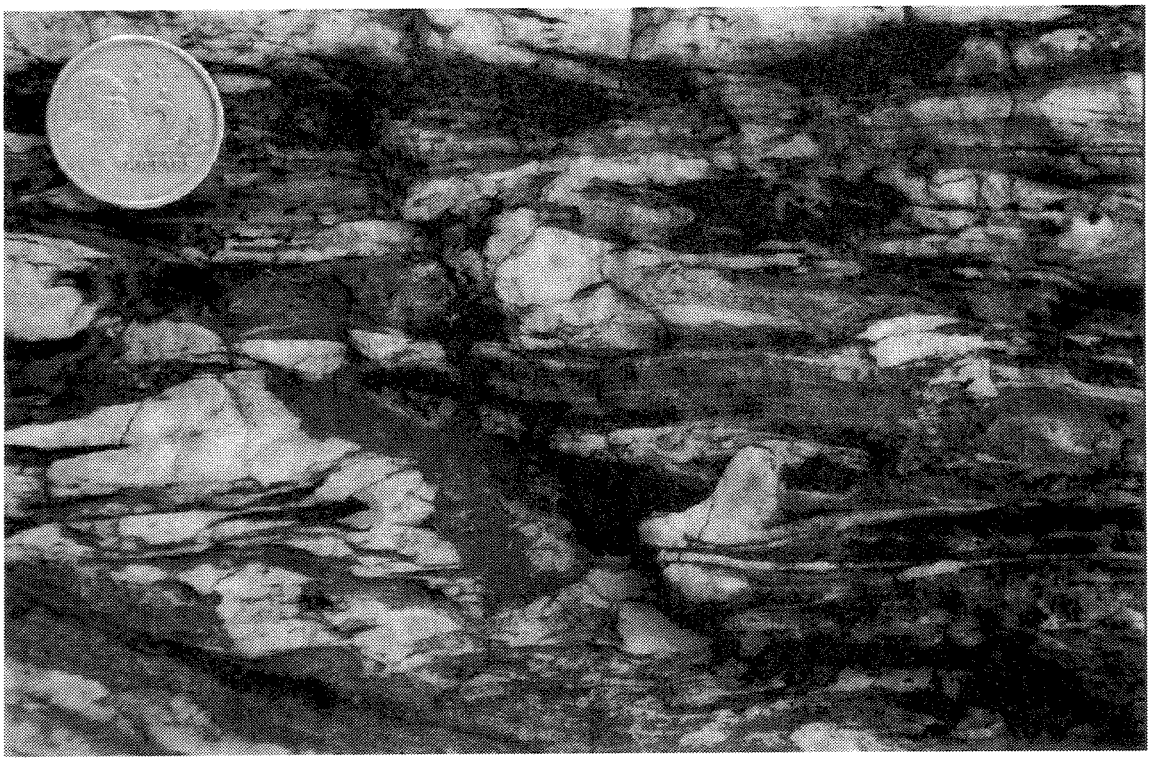

**Figure 5. Composite fabric in layered metachert in the Murphy Hills at Stop 1C. The rock contains a strong fabric with numerous tight to isoclinal, rootless $F_2$ fold hooks. View looking down onto a horizontal surface approximately perpendicular to $S_0$ and $S_2$**

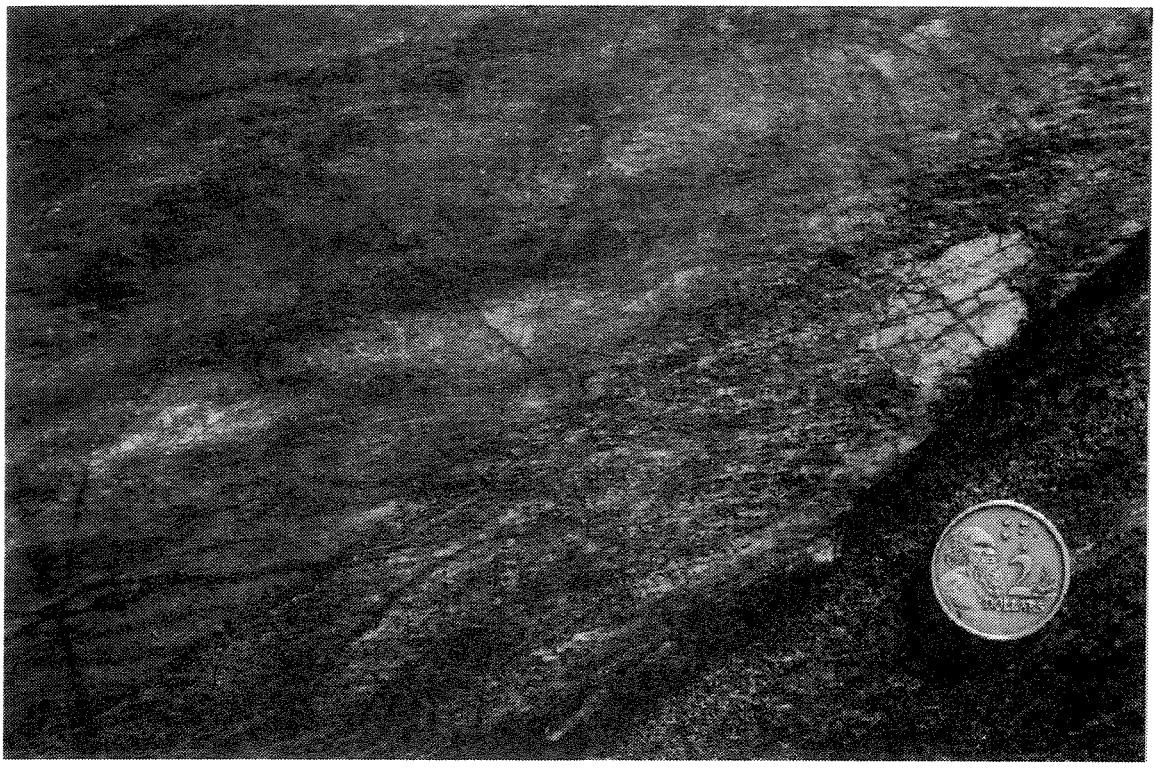

SW 38 27.08.97

**Figure 6. Overprinting lineations in a layered metachert in the Murphy Hills at Stop 1C. The rock has a steeply pitching, coarse lineation ($L_2$) resulting from the intersection of $S_0$ and $S_2$. This lineation is overprinted by a fine, micaceous, shallow-pitching lineation ($L_3$). View looking west onto a steeply dipping $S_2$ surface**

of bedding and $S_2$ (Fig. 6). These fabrics are in turn folded about shallow north-plunging axes into open, concentric $F_3$ folds (Fig. 7). There is an associated fine, combined mineral/crenulation lineation that is parallel to the fold axes (Fig. 6). The two sets of structures ($D_2$ and $D_3$) have distinct and consistent differences in style and orientation.

Both generations of structures are postdated by sporadically distributed, small-scale kink folds and crenulations ($D_4$). There is a possibility that there is an early, bedding-parallel, $S_1$ fabric in these rocks but it is difficult to identify due to the intensity of the $D_2$ deformation event.

## Stop 1D: Gneiss–greenstone contact — AMG 51J 4222 69059

The rocks at the greenstone margin in this location are intensely deformed. Quartzofeldspathic gneisses and greenstones both have a well-developed, planar fabric that dips steeply to the east

**Figure 7. Upright, concentric, shallow-plunging $F_3$ fold in a layered metachert in the southern part of the Murphy Hills. Profile view facing north. Located south, along strike, from Stop 1C**

(probably combined $S_2/S_3$). The gneisses contain two overprinting lineations, similar to those in the layered metachert at Stop 1C. The earliest lineation ($L_2$) is coarse, steeply plunging and is defined by the intersection of $S_1$ and $S_2$. It is overprinted by a shallow-plunging mineral lineation ($L_3$) defined by the alignment of fine-grained white mica. The greenstones at the contact are dominated by fine-grained amphibolite/metabasalt with a well-developed foliation and a prominent, steeply to moderately plunging mineral lineation, which is defined mainly by the alignment of hornblende.

The contact between the two rock units is strongly deformed, with the highest strain at the contact. The difference in orientation between intersection lineations in the greenstones (average 62°→130°) and gneisses (average 67°→028°; Fig. 3) suggests either that there was a structural discordance between the two units prior to $D_2$, or that they are on opposite limbs of an $F_3$ fold.

### Stop 1E: Granite–greenstone contact — AMG 51J 4210 69092

At this location there is a weathered exposure of the actual contact between a granitoid and the greenstones. The granitoid is weakly deformed and cuts across the foliation in the greenstones. The interpretation of these relationships is that the fabric in the greenstones is $S_2$ and that the granitoid is post-$D_2$. At this exposure the strain is low, but granitoids nearby contain a well-developed $S_3$ foliation with a shallow-pitching mineral lineation, illustrating the heterogeneity of strain in $D_3$.

## Locality 2: Banjawarn — Dingo Range greenstone belt

### by T. R. Farrell

Greenstone sequences at the southern end of the Dingo Range greenstone belt have undergone high-grade metamorphism and partial melting, and are extensively intruded by granitoids. Greenstone remnants in the granitoids range from small xenoliths, less than 10 mm in length, to large rafts up to 2.5 km in length (Fig. 8). The southern part of the greenstone belt contains a layered sequence dominated by amphibolite with numerous thin layers of felsic rock and tremolite–chlorite schist. Metamorphosed pyroxenite, melanocratic gabbro and peridotite are minor constituents of the sequence. The amphibolites are finely layered in many areas and have a strong composite fabric ($S_1/S_2$), with rootless $F_2$ fold hooks, and a prominent, combined intersection/mineral lineation parallel to the fold axes. $F_2$ folds are upright and plunge to the north at about 40–50°. The composite fabric is overprinted by a fine, shallow-plunging mineral lineation and small upright, shallow-plunging $F_3$ folds.

Granitoids in the Banjawarn area contain abundant enclaves of high-grade mafic rocks, quartzofeldspathic gneiss and serpentinized peridotite. The proportions of granitoid and gneiss are uncertain due to the lack of outcrop, but the area may be underlain by large areas of multiply deformed gneiss with multiple injections of granitoid. The main granitoid type is a fine-grained biotite monzogranite. In some parts, it has a strongly developed foliation and a north-plunging mineral lineation. These structures are similar in orientation to equivalent structures ($D_2$) in the greenstones, which suggests that some of the granitoids were intruded prior to $D_2$. These granitoids may be an earlier phase of magmatism, associated with the formation of the gneisses, that is separate from the main phase of granitoid magmatism in $D_2$.

The purpose of the stops in this area is to examine the high-grade metamorphic rocks at the southern end of the Dingo Range greenstone belt.

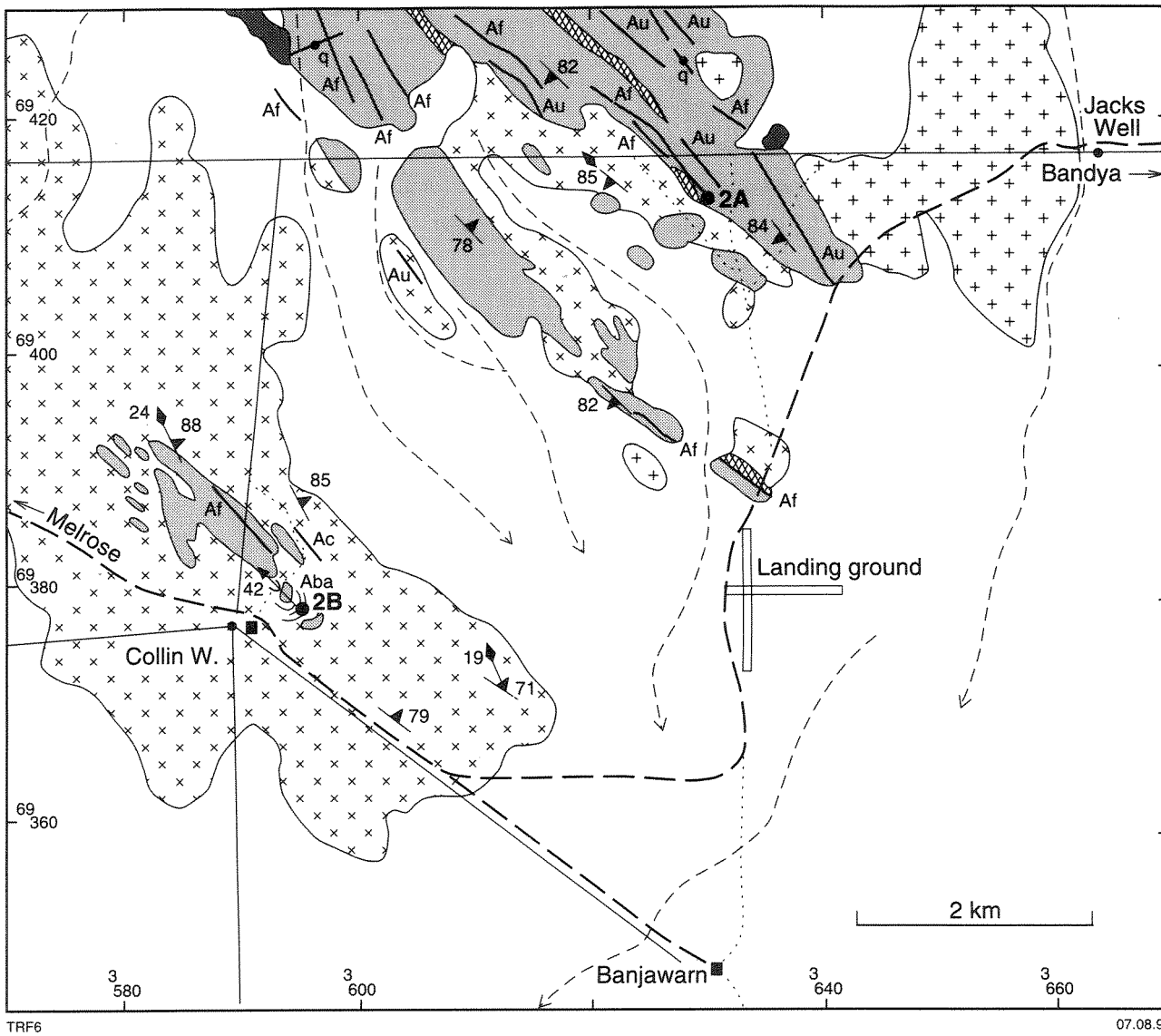


CAINOZOIC

- Transported regolith, undivided
- Lateritic duricrust

ARCHAEAN

- q — Quartz vein
- Granitoid rock, mainly monzogranite
- Granitoid and quartzofeldspathic gneiss
- Ac — Chert and layered chert, metamorphosed
- Af — Metamorphosed felsic rock, undivided
- Aba — Amphibolite
- Au — Metamorphosed ultramafic rock, undivided

Dominant foliation, showing strike and dip

- 72 inclined

Lineation, showing trend and plunge

- 19 mineral lineation, association uncertain

Fold axis, showing trend and plunge

- 60 $F_2$ fold, symmetric
- Road
- Track
- Fence, generally with track
- Homestead
- Well
- Watercourse, ephemeral
- 2A Excursion stop

**Figure 8. Outcrop geology of the Banjawarn area**

### Stop 2A: High-grade layered sequence — AMG 51J 3628 6916

At this stop there is a high-grade, strongly deformed, layered sequence of amphibolite, felsic schist and tremolite–chlorite schist. The greenstones form an elongate, finger-like projection into the granitoids and gneisses. The rocks show evidence for at least two phases of deformation. They have a well-developed composite foliation ($S_1/S_2$) with a prominent north-pitching mineral lineation ($L_2$). A later, fine-grained, shallow-pitching lineation ($L_3$) overprints the $L_2$ lineation in some rocks. To the southwest, the greenstones are in probable intrusive contact with a granitoid that contains abundant rafts of amphibolite and metagabbro.

### Stop 2B: Fold hinge in a greenstone remnant — AMG 51J 3595 6937

At this stop, there is an exposure of an $F_2$ fold hinge in a greenstone remnant in the granitoids and gneisses. Layered pyroxene-bearing amphibolites contain a strong composite $S_1/S_2$ fabric with dismembered $F_2$ folds. In the hinge zone, $S_1$ and $S_2$ are at a high angle to each other and both are defined by high-grade assemblages of hornblende, plagioclase, clinopyroxene, quartz, sphene and ilmenite. The fold is outlined by refractory layers of amphibolite in biotite monzogranite and the fold axis plunges at about 40° to the northwest.

## Locality 3: Wadarrah Quartz Monzonite — Rosewood Well — AMG 51J 3352 6917

**by S. Wyche**

The Wadarrah Quartz Monzonite is a hornblende–quartz monzonite that forms tors and whalebacks northeast of the Darlot mine site. It is a pink, medium- to coarse-grained porphyritic rock with alkali feldspar phenocrysts averaging 10 mm in diameter, but with some elongate plagioclase phenocrysts up to 40 mm long. The abundance of these phenocrysts varies markedly. Narrow quartz veins and aplite and pegmatite dykes are common. The quartz monzonite is relatively massive although a locally prominent fabric, probably a flow foliation, is defined by the alignment of hornblende and biotite crystal aggregates. The pluton contains xenoliths of greenstone, tens to hundreds of metres across, which are cut by granite, aplite and pegmatite dykes.

The Wadarrah Quartz Monzonite contains quartz, microcline, plagioclase, biotite (some of which is altered to chlorite), hornblende, abundant euhedral titanite and apatite, epidote and magnetite. There is also minor fluorite, commonly associated with biotite. The rock is partly

recrystallized and contains strained quartz showing undulose extinction and some local granulation.

At the excursion stop, just east of Rosewood Well, the contact between the quartz monzonite and the adjacent greenstone sequence is a zone, about 100 m wide, where stringers of granitoid are interlayered with metabasalt on a scale of 1 to 100 mm. Basalt along the contact has been metamorphosed to amphibolite facies, and is noticeably higher grade than metabasalt in the adjacent greenstone sequences. Granitoid and pegmatite dykes up to 3 m wide intrude greenstones parallel to the contact. Both granitoid and amphibolite are moderately to strongly deformed along the contact, indicating that significant deformation took place subsequent to granitoid intrusion, probably during the regional $D_3$ event.

The Wadarrah Quartz Monzonite has a U–Pb zircon age of 2643 ± 6 Ma (Nelson, in prep.). This relatively young age and the apparent intrusive relationship between the monzonite and greenstones suggest that the Wadarrah Quartz Monzonite was intruded late in the $D_2$–$D_3$ deformation regime.

## Locality 4: Bedded felsic volcaniclastic rocks — Katherine Well — AMG 51J $_{3}$223 $_{69}$415

### by S. Wyche

Bedded, crystal-rich, felsic rocks are abundant in an area between 4.5 and 6.5 km east of Katherine Well (Westaway and Wyche, in prep.). These rocks typically form deeply weathered float and bleached pavements. However, 6 km east-northeast of Katherine Well, there are fresh outcrops along a ridge 1.7 km in length. Two smaller fresh outcrops also occur along strike to the south of the ridge (Fig. 9). The outcrops consist of large boulders and tors up to 4 m high. They are locally foliated and jointed, with some boulders slightly lens shaped and oriented in the direction of the foliation.

Larger outcrops are massive to bedded, and pale cream to buff in colour. Bedding appears as diffuse greyish bands that vary from 20 to 100 mm in thickness, with an average of 40 mm (Fig. 9). In places there is slight differential weathering of the darker bands, possibly reflecting a subtle compositional variation. Facing directions can be determined from graded bedding in thicker bedded units in some bleached pavements.

**Figure 9. Bedding in immature volcaniclastic rock from outcrops 4.5 km south-southwest of Locality 4**

In thin section, the volcaniclastic rocks are crystal rich with grains of quartz and lesser amounts of sericitized plagioclase, K-feldspar and altered lithic fragments comprising up to 50% of the rock. They are set in a very fine-grained recrystallized quartzofeldspathic groundmass. Epidote and leucoxene are common accessory minerals. The grains are angular, poorly sorted, and range up to 3 mm. Individual grains are anhedral to euhedral with abundant broken crystals — some with jigsaw-fit texture. There is no evidence of welding.

The diffuse nature of the bedding and the textural and mineralogical immaturity of these rocks indicates that there has been very little reworking. They probably represent a pyroclastic fall deposit associated with the Spring Well felsic complex.

## Locality 5: Bronzewing gold mine

### by J. Landmark

The discovery of the Bronzewing gold deposit in 1992 (Fig. 10), within the Yandal greenstone belt, epitomizes the successful search for new resources under cover and represents a significant advance in exploration for Australian gold deposits. Bronzewing has a mineral resource estimate of some 38.3 Mt at an uncut grade of 2.92 g/t Au (December 1996). Detailed descriptions of the Bronzewing deposit are given by Eshuys et al. (1995), Eshuys and Lewis (1995), Phillips et al. (1996), and Phillips et al. (in press).

A combination of a good geological appreciation of the exploration potential of the Yandal belt, an understanding of the regolith-forming processes and drilling programs using appropriate techniques have led to the development of one of Australia's largest recent gold discoveries.

### Regional geology

The Bronzewing area is dominated by a broad alluvial plain of lateritized and indurated sediments overlying a deeply weathered volcanic sequence that is composed of metabasalt, some ultramafic rocks and rare metasedimentary rocks. Fresh rock is 120 m below surface. The dominant host rock for gold mineralization is metamorphosed tholeiitic basalt (and its sheared equivalent). Basaltic textures vary from obvious pillows to thick medium-grained equigranular flows that are difficult to distinguish from dolerite. Within the mine environs there are two major intrusive bodies. To the west there is a northerly trending ultramafic to mafic sill, and granodiorite occurs on the eastern side of the Discovery pit.

The Bronzewing orebodies lie to the west of the Hook antiform (a regional-scale, southerly plunging structure) and are contained within a series of north-trending ductile shear zones. The host rocks to mineralization are variably sheared with an overall strike direction of 360° (and dip of 70° east). In detail, however, the shear zones are anastomosing, wrapping around boudins of less-deformed material on all scales. The regional metamorphic grade in the area is mid- to upper greenschist facies.

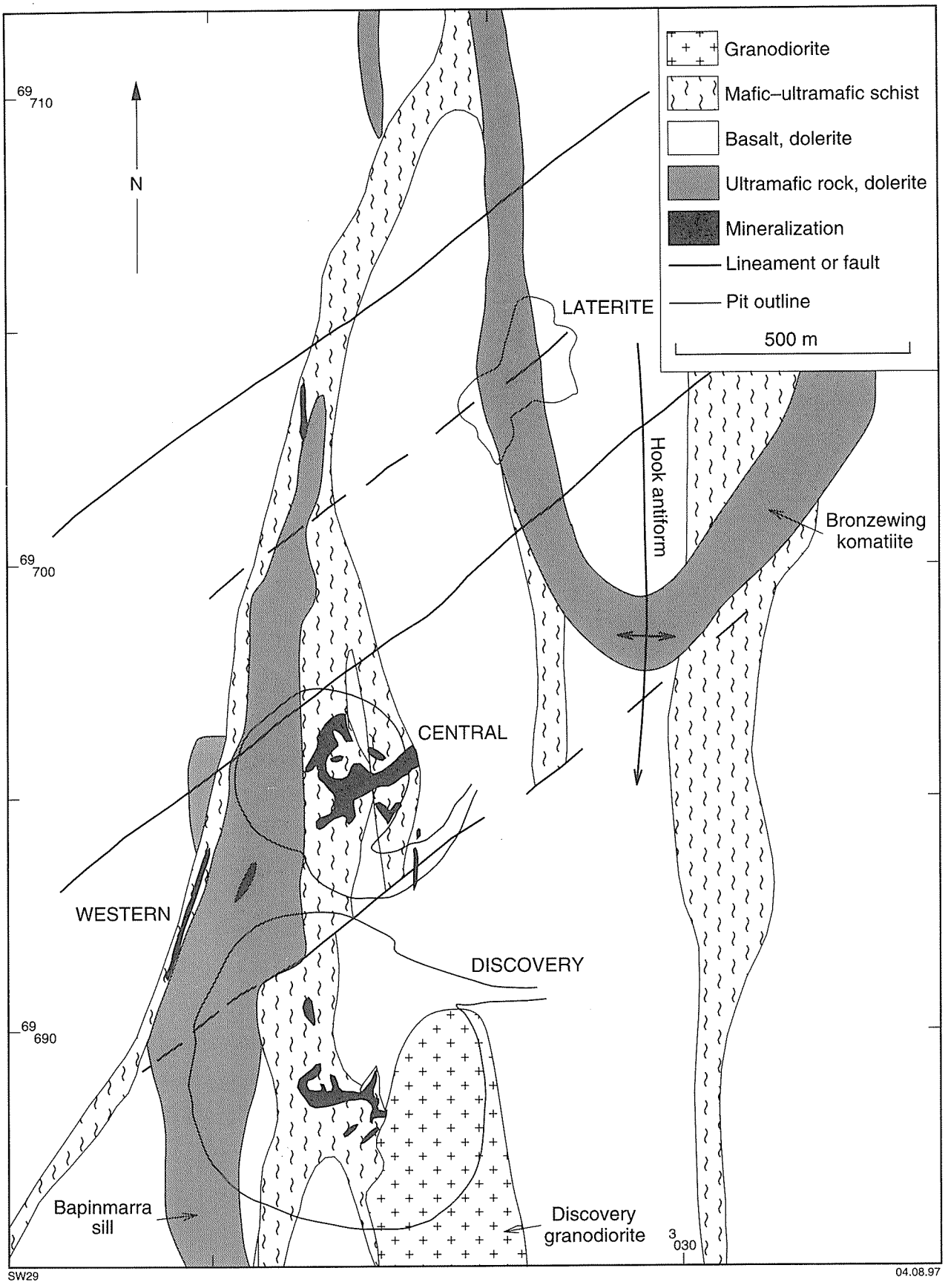


**Figure 10. Geology of the Bronzewing area**

## Mineralization

Gold mineralization is associated with quartz veining and is hosted in quartz veins and stockworks within potassium-enriched alteration zones, predominantly within variably sheared basalt. Mineralization is currently outlined within a zone 2 km long, 500 m wide and at least 800 m deep.

Vein mineralization and alteration are typically in two forms, as described below.

### *Central Zone (Shoot 39)*

Central Zone mineralization ranges from isolated quartz veins confined within narrow shears, in the upper parts of the system, to a zone of intense, closely spaced quartz veining. This zone is 5 to 80 m wide, up to 130 m in strike length, and has a southerly, down dip extent of greater than 400 m. Veining is accompanied by muscovite–carbonate–biotite–pyrite–chlorite alteration ranging from narrow selvages to pervasive zones tens of metres wide. The main bulk of the Central Zone (referred to as Shoot 39) trends northeast and dips steeply to the southeast.

Contained within the core of the Central Zone, from about 5 Level down to at least 8 Level, there is a massive and relatively undeformed quartz vein up to 15 m wide, informally known as the Herbie vein. This vein is highly auriferous and is dominantly massive to weakly laminated. Coarse-grained, free gold is locally abundant within this vein, which also contains chalcopyrite, scheelite and tellurides as common accessory minerals. Overall, the Herbie vein mirrors the shape of the enclosing mineralization/alteration envelope.

Mineralization within the Discovery pit is similar to that of the Central Zone.

### *Western Zone*

The Western Zone is a narrow, folded quartz vein from 0.1 to 5 m wide and up to 250 m long that contains abundant free gold associated with chalcopyrite and Bi–Ag tellurides. Gold is located within narrow laminar zones that parallel vein margins. The vein system postdates an unmineralized footwall and/or hangingwall quartz breccia, all of which is enveloped by a mafic–ultramafic schist up to 50 m wide and striking at about 030°. The breccia is composed of fragments of biotite–pyrite-altered basalt up to 2 m in length.

Throughout all mineralized zones at Bronzewing there is commonly an association between the presence of sulfides (in particular chalcopyrite, but also pyrite and pyrrhotite) and higher grades of gold, even though the total sulfide content is low. Scheelite is also a good indicator of high grades. Gold occurs both as free grains and as small inclusions within pyrite, but it is all free milling. The fineness averages about 920. The percentage of telluride in the ore also affects the fineness of the gold bars produced.

## Locality 6: Granite–greenstone contact — Mount McClure — AMG 51J $_{2}$955 $_{69}$522

### by S. Wyche

A strongly deformed and metamorphosed zone along the western side of the Yandal greenstone belt is up to 13 km wide, and comprises complexly interleaved granitoid, gneiss and greenstones. This zone is characterized by shallow to moderate easterly and westerly dipping foliations with local mylonitic zones. There is a strongly developed mineral lineation that typically has a shallow southwards plunge, but is locally horizontal to north-plunging. Rocks within the greenstone sequence adjacent to this zone have attained a higher metamorphic grade than those in the adjacent greenstone sequences. Mafic rocks at the contact, and in the interleaved zone immediately to the west, are metamorphosed at greenschist to amphibolite facies, whereas those within the Yandal greenstone belt to the east are mainly greenschist facies rocks. The shearing at the contact can be attributed to the regional northerly to northwesterly trending deformation event ($D_3$; Farrell, 1995; Wyche and Westaway, 1995). This is consistent with observations of granitoid–greenstone contacts in areas to the south (Swager and Nelson, 1997). Other parallel structures, suggested by discontinuities in aeromagnetic images and structures that host gold mineralization in the Mount McClure deposits, may also be related to this deformation event.

A SHRIMP U–Pb age determination on a sample of granitoid gneiss from the northern side of the road to Bronzewing indicates a crystallization age of 2738 ± 6 Ma for the felsic precursor to the gneiss (Nelson, in prep.). This age is significant because it is older than any age determined on greenstones from within the Norseman–Wiluna greenstone belt. Felsic volcanic rocks from near Norseman dated at 2930 ± 4 Ma (Nelson, 1995) are interpreted as belonging to an older greenstone sequence, perhaps equivalent to those in the Southern Cross Province (Swager et al., 1995). The gneiss at Mount McClure probably represents felsic magmatism associated with the early development of the 'Norseman–Wiluna basin' rather than sialic basement to the greenstone succession. Abundant evidence from xenocrystic zircons from throughout the Eastern Goldfields

Province suggest that greenstones were deposited on a sialic basement possibly greater than 3.0 Ga old (e.g. Compston et al., 1986; Nelson, 1995, 1996, 1997, in prep.).

## Locality 7: Spring Well felsic volcanic complex

### by S. Wyche

The volcanic centre of the Spring Well felsic volcanic complex (Giles, 1980, 1982; Westaway and Wyche, in prep.) is situated in the vicinity of Spring Well (Fig. 11). Here an assortment of felsic volcanic, volcaniclastic and high-level intrusive rocks ranging in composition from rhyolite to basaltic andesite form outcrops in a group of low hills and ridges. Rocks around Spring Well are described as igneous rocks because they are little deformed or metamorphosed. The rocks are typically fresh and preserve a wide range of primary igneous textures. Away from the volcanic centre, the range of volcanic textures is limited, with finer tuffs and tuffaceous sedimentary rocks predominant and fine-grained volcaniclastic rocks more abundant. It is suggested that the Spring Well complex represents a continental stratavolcano, because of the lateral lithological and compositional changes, the high proportion of pyroclastic rocks, and the large volume of volcanic breccias near the volcanic centre.

Nelson (1997) has obtained an age of 2690 ± 6 Ma for porphyritic rhyolite from Spring Well. This age is similar to ages for calc-alkaline volcanic complexes in the southern part of the Eastern Goldfields Province (Nelson, 1995, 1996).

Hallberg and Giles (1986) compared the geochemistry of a number of felsic volcanic centres in the northeastern part of the Yilgarn Craton and concluded that the Spring Well complex is one of a series of calc-alkaline rock suites whose primary magmas were derived by shallow, hydrous partial melting of large-ion lithophile element(LIL)-enriched mantle.

There are good exposures in the Spring Well district of a range of volcanic rocks including fine- to medium-grained intermediate rocks, rhyolitic and dacitic lavas, lapilli tuff, and coarse volcanic breccia.

The **intermediate rocks** range in composition from basaltic andesite to andesite. Outcrops are typically dull grey-green and grey in colour and consist of rounded boulders, either in isolated hills, or in recessive areas between outcrops of resistant, more siliceous units. Although commonly fine- to very fine-grained, the intermediate rocks are locally porphyritic and glomeroporphyritic, with phenocrysts of plagioclase and/or clinopyroxene, in places up to 5 mm in diameter. Some of the

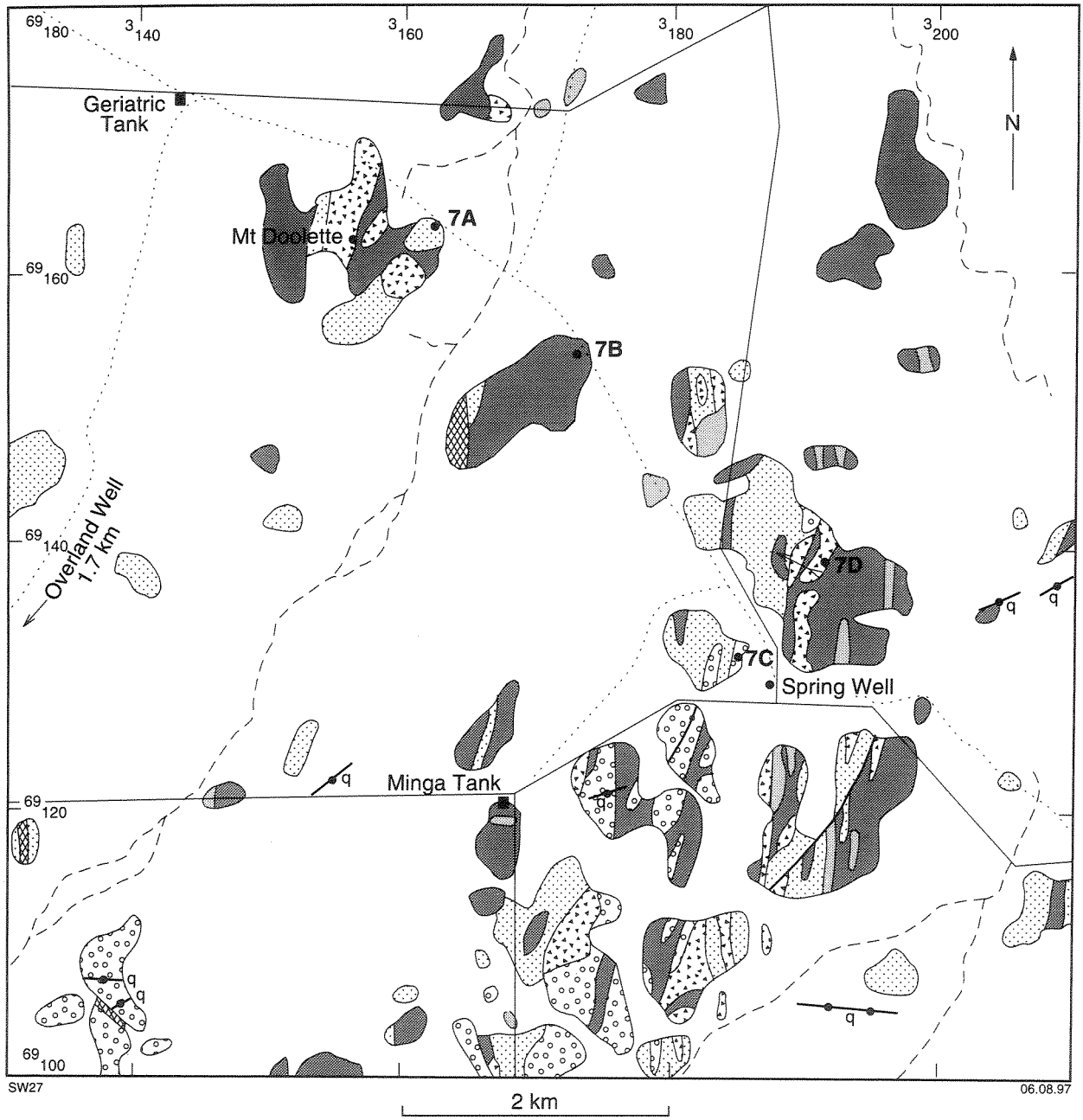


**Figure 11. Geology of the Spring Well district (after Wyche and Westaway, 1996)**

very fine-grained material contains devitrified glass. Plagioclase is the most abundant constituent, both as a phenocryst phase and as a fine-grained phase. Finer grained plagioclase occurs as laths and microlites. The grains typically have a random orientation, but are weakly aligned in places, and a pronounced trachytic texture is locally developed. Clinopyroxene is common, both as a fine-grained phase and as phenocrysts in porphyritic rocks. It is commonly altered to amphibole and chlorite but pseudomorphs of coarser phenocrysts, locally up to 5 mm long, have clear crystal outlines. Quartz is a primary phase in some of the fine-grained varieties. Pale-green amphibole replaces clinopyroxene and occurs as fine acicular grains in some samples. Opaque oxide minerals are locally abundant, commonly with skeletal textures outlined by leucoxene. Secondary epidote-group minerals are common and there is local carbonate alteration.

In most cases, there is no clear field evidence to indicate whether the intermediate rocks are extrusive rocks or high-level intrusions of dioritic to granodioritic composition. No pillow structures have been seen in the Spring Well complex, but textures (e.g. locally developed trachytic texture) indicate that at least some of these rocks may have been extrusive. Although no lava flows have been recognized, amygdales are abundant locally, and range in size from 1–2 mm up to 70 mm in maximum dimension (described below at Stop 7B).

**Fine-grained felsic volcanic rocks** include both pyroclastic rocks and lavas, although it is not always possible to determine the style of deposition. The very fine-grained quartzofeldspathic groundmass may, in some instances, represent devitrified glass. Elsewhere the groundmass consists of very fine plagioclase laths that are randomly oriented, or aligned in an apparent trachytic texture. These rocks are porphyritic in places, with fine-grained quartz and plagioclase phenocrysts, and may contain small glomeroporphyritic aggregates of fine-grained plagioclase. The presence of broken crystals and glass shards in some specimens suggests a pyroclastic origin for much of this material. Spherulites are rare but devitrification textures including spherulites and perlitic cracks are preserved in some glassy clasts in the coarse volcanic breccia. Amygdaloidal varieties are present locally. Chlorite and epidote are common secondary minerals in these rocks, and calcite is present locally. Glassy rhyolite lavas with well-preserved flow banding and perlitic fractures have been mapped locally (described below at Stop 7A).

**Porphyritic felsic volcanic rocks** ranging in composition from rhyolite to dacite have been mapped mainly to the west and south of Spring Well (described below at Stop 7C). There are numerous fresh outcrops in which phenocrysts of plagioclase (commonly saussuritized) and quartz comprise from 10% to about 40% of the rock. Phenocrysts up to 3 mm across are embedded in a very fine-grained, probably recrystallized, felsic matrix. Plagioclase may be present as euhedral and broken crystals, and also as glomeroporphyritic aggregates. Quartz grains are typically anhedral, rounded, and embayed as a result of resorption. Some have thin reaction rims. Broken

quartz grains have a jigsaw-fit texture indicating in situ fragmentation. Epidote, chlorite and calcite are common secondary minerals.

The porphyritic felsic volcanic rocks may represent lavas, subvolcanic intrusions or pyroclastic deposits. Near Spring Well, where they form small hills and rocky outcrops, they are commonly associated with fine-grained tuffs and appear to be locally intruded by fine-grained intermediate rocks. These outcrops vary in overall phenocryst abundance and in the relative abundance of quartz and plagioclase phenocrysts.

**Lapilli tuff** is a widespread rock type in the Spring Well complex. It consists of a mixture of angular, poorly sorted, altered, devitrified, glassy volcanic clasts in a very fine-grained, felsic, devitrified glassy matrix. The tuff may also contain broken quartz and feldspar grains. The range of mainly fine-grained felsic clast types includes altered material that may represent original pumice fragments and glass shards. Compaction and welding is evident at both outcrop and microscopic scales. Flattening and alignment of clasts producing a eutaxitic texture is commonplace. In some outcrops, particularly those distal to the volcanic centre, there is a weakly developed layering that is probably also a primary feature.

**Coarse volcanic breccias** form prominent ridge cappings and isolated outcrops at Spring Well (Fig. 12), in the hills immediately to the south and southwest of Spring Well, and at Mount Doolette. These rocks are generally poorly sorted and matrix-supported, and contain a range of volcanic clast types, including volcanic glass, flow-banded rhyolite, porphyritic rhyolite and dacite, and individual quartz and feldspar grains. Aphanitic and finely porphyritic rhyolitic to dacitic volcanic rocks are the most abundant clast types. Intermediate clasts are rare or absent. Outcrops generally have no internal stratification or bedding. Both clasts and matrix commonly contain epidote and chlorite. Some outcrops may have undergone secondary silicification.

Clasts in the volcanic breccias are angular and typically less than 100 mm across, but may range up to more than 300 mm long. Boundaries between clasts and the enclosing matrix are generally sharp. However, some glassy fragments in the breccia do have thin reaction rims, perhaps 1 to 2 mm thick (Fig. 13). Bunting and Williams (1979) interpreted the rims as evidence for the incorporation of cold fragments into a hot matrix. The presence of perlite and broken crystals in the matrix, vitriclastic textures, and evidence of welding and flattening of glassy clasts in outcrops immediately north of Spring Well supports Giles' (1980, 1982) interpretation of these rocks as pyroclastic deposits proximal to the volcanic centre. However, these features are not seen in all exposures and it is possible that some of the breccia units were deposited as debris flows adjacent to active volcanoes.

**Figure 12. Coarse volcanic breccia 1 km north of Spring Well with angular clasts of mainly rhyolitic to dacitic composition in a fine, devitrified, glassy matrix**

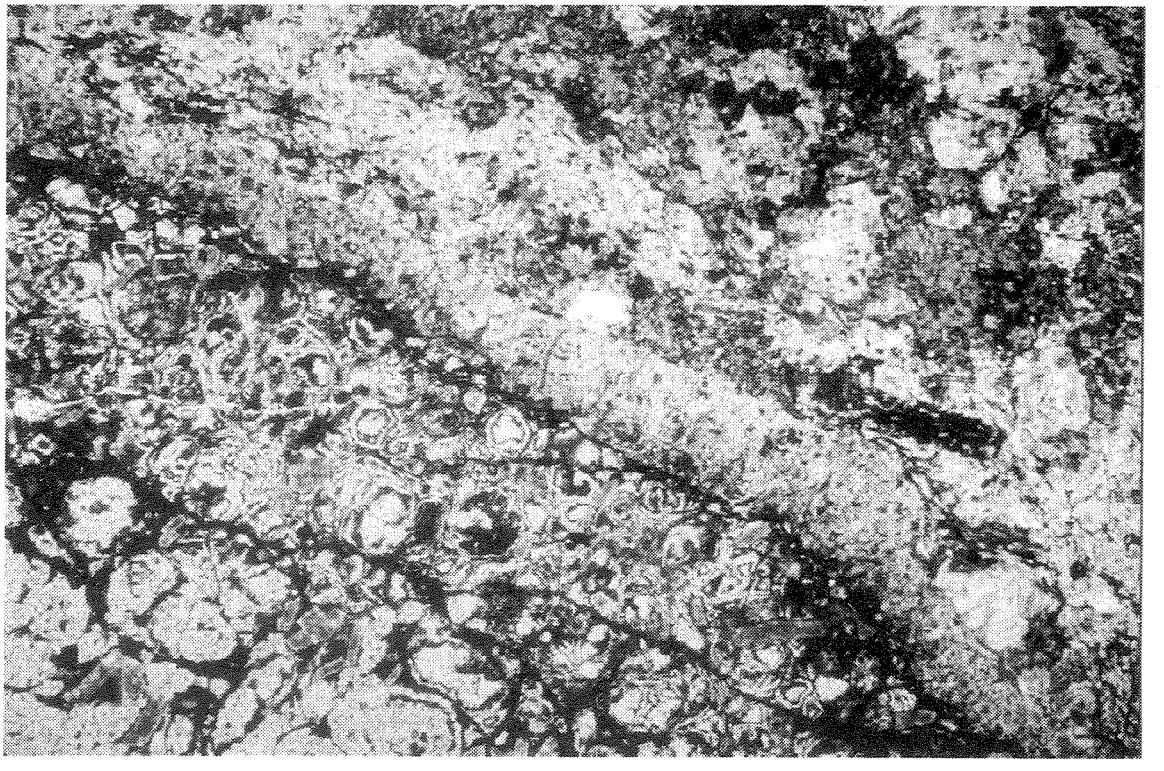

**Figure 13. Reaction rim on glassy clast in coarse volcanic breccia from 1 km north of Spring Well: relict perlite fractures in the matrix. GSWA 121724, plane-polarized light. Field of view is 6.5 mm**

## Stop 7A: Mount Doolette — AMG 51J 3162 69162

At Mount Doolette, there are good exposures of a range of the typical rock types exposed in the Spring Well area.

The ridge on the southeastern side of the Mount Doolette area contains a well-preserved rhyolite sequence displaying a variety of textures. Rhyolite lava on the hill at the eastern end of the ridge forms a glassy autobreccia, with angular clasts up to 200 mm in diameter, with very well-preserved flow banding. On top of the hill, an outcrop of very fine-grained siliceous rock contains a diffuse, regular layering on a scale of about 30 mm. This layering resembles bedding and the outcrop may be an ash-fall deposit. However, the association with nearby coherent rhyolite lava suggests that this texture may be a planar flow foliation. Much of this hill has the texture of a matrix-supported breccia with distinctive, uniform angular 'clasts' up to 50 mm in diameter. This texture probably represents large perlitic fractures (macro-perlite) in a coherent rhyolite lava (McPhie, J., 1997, pers. comm.).

Much of the ridge appears to be intruded by grey intermediate rocks, typical of those throughout the district (as described above).

Farther to the southwest, along the ridge, across the intermediate unit, and on the prominent ridge approximately 400 m to the west, there are extensive outcrops of coarse volcanic breccia (see above).

## Stop 7B: Intermediate rock south of Mount Doolette — AMG 51J 3173 69154

This stop allows examination of large amygdales, in an intermediate rock, that range in size from 1 to 2 mm up to 70 mm in maximum dimension. They are typically filled with quartz but may contain calcite, epidote and/or chlorite. The locally abundant presence of amygdales suggests that these rocks are extrusive or, at least, high-level intrusive rocks.

## Stop 7C: Flow-banded porphyritic dacite/rhyolite — AMG 51J 3185 6913 2

The excursion stop lies within a discontinuous line of outcrops in the hills 500 m to the west of Spring Well. Here, porphyritic rock of rhyolitic to dacitic composition displays well-preserved, strongly contorted flow banding with local autobrecciation (Fig. 14). These outcrops were interpreted by Giles (1980, 1982) as rheoignimbrite: an ignimbrite that has flowed while still in a plastic state. However, it is more likely that this material represents a lava flow of rhyolitic to dacitic composition. Farther west, in the area southeast of Overland Well, relatively fresh felsic porphyritic rocks (similar in character to the less quartz-rich types near Spring Well) outcrop over an area of several square kilometres. They are massive, homogeneous, and lack any internal structure including bedding or layering. Giles (1980, 1982) interpreted these rocks as crystal tuffs.

## Stop 7D: Spring Well section — AMG 51J 3189 6914 0

The section through the hills immediately north of Spring Well traverses a representative range of the rock types encountered in the region and it includes some spectacular outcrops of coarse volcanic breccia, in addition to a range of tuffs and lavas.

**Figure 14. Flow banding in porphyritic rhyolite 800 m southwest of Spring Well**

Intermediate rocks at the eastern end of the traverse are like those elsewhere in the Spring Well area. At this location, some of the intermediate rocks have a patchy texture that weathers to form shallow hollows up to 30 mm in diameter. These appear to be secondary features and may be a reflection of varying degrees of epidotization.

The traverse over the top of the ridge to the west, covers a range of mainly acid volcanic rock types, including coarse volcanic breccia, lapilli tuff, and fine-grained, glassy volcanic rocks with various crystal contents. These rocks appear to be locally intruded by the grey intermediate rocks.

Coarse volcanic breccia (see above) forms a cap on the top of the main ridge at this locality (Fig. 12). Outcrops of the coarser material generally have no internal stratification or bedding. However, an overall fining-up across the top of the ridge and some local-scale graded bedding in crystal-rich units indicate a westward younging direction (Giles, 1980, 1982).

## Locality 8: Lawlers Anticline — AMG 51J 2559 68950

### by S. F. Liu and S. Wyche

At Locality 8 there is clear evidence of two episodes of deformation — an early shallow north-dipping foliation with a shallow north-plunging mineral lineation has been folded around the Lawlers Anticline.

The Lawlers Anticline, described in detail by Platt et al. (1978), is an upright, shallow, north-plunging fold in a greenstone sequence comprising metamorphosed gabbro, basalt, ultramafic and minor sedimentary and felsic volcanic rocks (Fig. 15). This sequence is bounded on its western side by a major regional ($D_3$) shear zone, the Waroonga Shear. Close to the Waroonga Shear, the Jones Creek Conglomerate is represented by a thick sequence of arkosic sandstone and conglomerates (Fig. 2).

The core of the anticline is occupied by the Lawlers Tonalite. Leucogranite intrusions occur along the contact between the greenstone sequence and the tonalite, but they do not contain the early shallow-dipping fabric present in both the greenstones and the tonalite, and so probably postdate the early deformation (Platt et al., 1978).

Platt et al. (1978) attributed isoclinal folds on the west limb of the Lawlers Anticline to $D_1$. They argued that their $D_1$ deformation produced a regional penetrative deformation to which they assigned the bedding-parallel foliation at this locality. A second foliation (a spaced cleavage, $S_2$) is

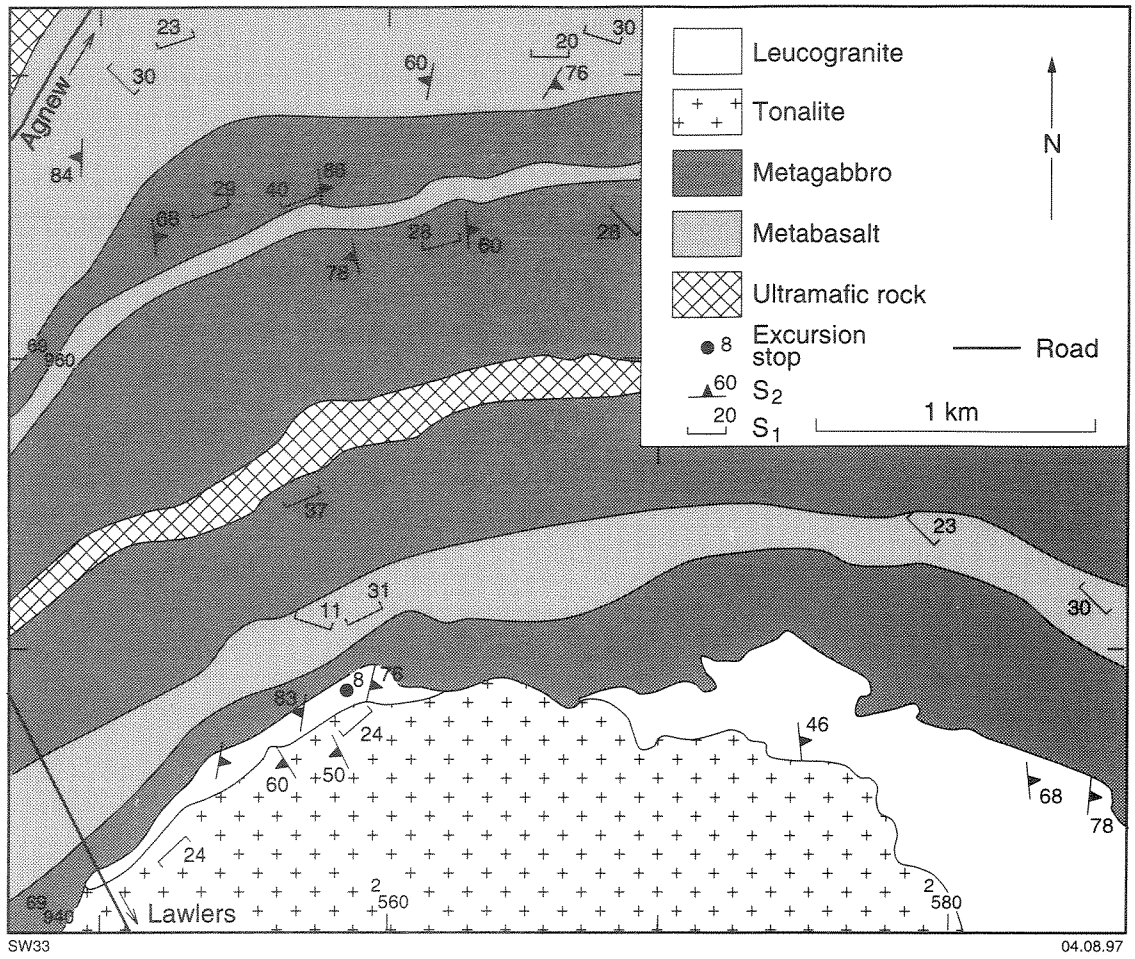


**Figure 15. Structural map of the hinge area of the Lawlers Anticline (after Platt et al., 1978)**

axial planar to the open, upright Lawlers Anticline. In the greenstones, this cleavage is defined by narrow (1 mm) zones of hornblende or chlorite that cut across the early fabric (Platt et al., 1978). This foliation is also present in the tonalite and the leucogranite. At this locality, the axial planes of upright folds in quartz veins in the leucogranite are parallel to the axial plane of the Lawlers Anticline, which suggests that they were formed during $D_2$.

## Locality 9: Lake Miranda — AMG 51J $_{2}$594 $_{69}$375

### by S. F. Liu

At the southeastern end of the elongate island in Lake Miranda, 3 km south of Bellevue gold mine, the tholeiitic Mount Goode Basalt is moderately to strongly deformed, with a well-developed, almost vertical, north-trending foliation, which is defined by the alignment of plagioclase and

amphibole. A major north-northwesterly trending shear zone, the Highway Fault, has been interpreted as passing through the lake, immediately west of this locality (Fig. 2; Liu et al., 1996).

In beach outcrops on the southeast corner of the island, pillow structures in metabasalt were deformed during the earliest recognizable deformation (Fig. 16). $S_1$ is defined by flattened pillows and the alignment of plagioclase phenocrysts. It is subvertical and trends to the north-northeast. The flattened pillows are overprinted by a strong regional deformation ($D_2$) that produced a prominent steep, subvertical, north-trending foliation (Fig. 17). The asymmetric shape of pressure shadows around plagioclase phenocrysts indicates a sinistral shear sense.

In the northeastern part of the same island, about 200 m north of the pillow basalt location, the $S_2$ foliation and a felsic porphyry dyke have been folded during $D_3$ to produce upright folds (Fig. 18) and a spaced crenulation cleavage ($S_3$), which is axial planar to the folds (Fig. 19). The $S_3$ crenulation trends to the northeast (at about 330°) and is very close to the regional $S_2$ foliation in orientation. Mineral segregation has resulted in pale and dark layers along $S_2$ (Fig. 19).

A later deformation ($D_4$) produced easterly trending fractures that are filled with quartz and have dark alteration zones containing amphibole. These fractures outcrop in the deformed pillow basalt at the southern end of the island.

SW 37 27.08.97

**Figure 16. Flattened pillow structures ($S_1$) in metabasalt near the north shore of Lake Miranda**

**Figure 17. Prominent foliation ($S_2$) and asymmetric pressure shadows around plagioclase phenocrysts in the metabasalt of Figure 16 (pencil is 8 mm in diameter)**

**Figure 18. Upright $F_3$ fold in metamorphosed felsic porphyry in metabasalt near the north shore of Lake Miranda**

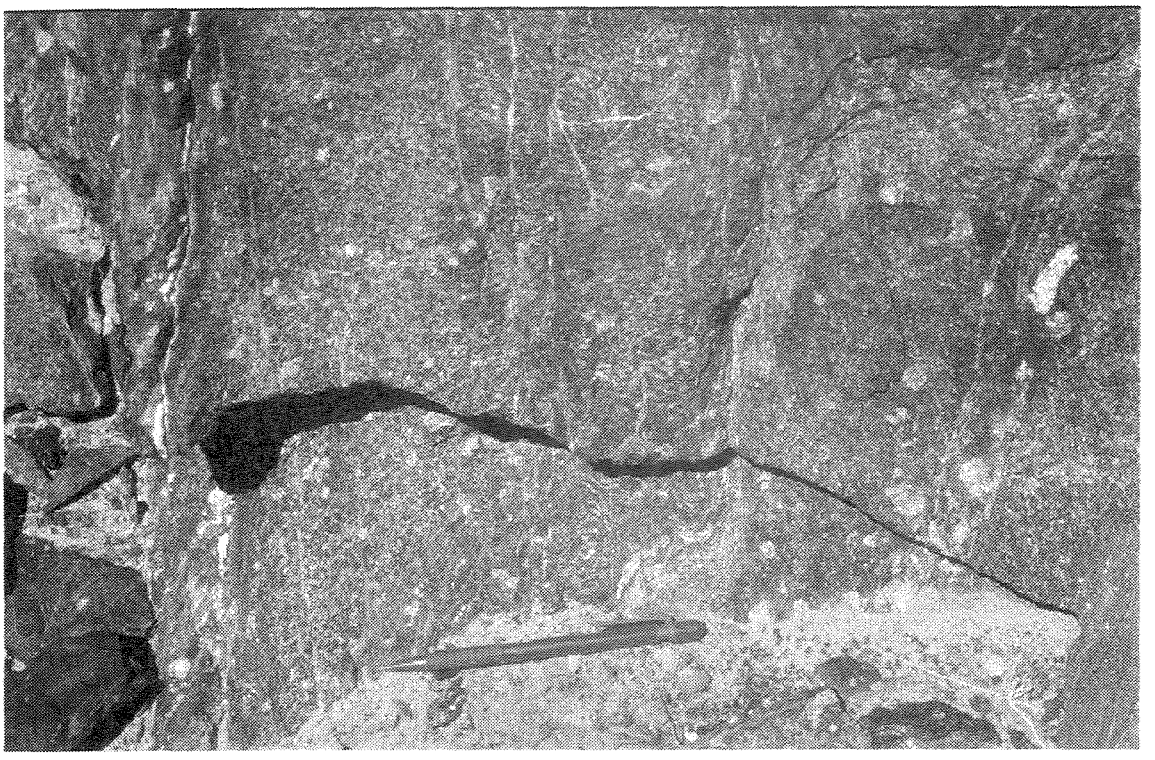

**Figure 19. Upright crenulation cleavage ($S_3$) and a flat-lying earlier foliation ($S_2$) in metabasalt near the north shore of Lake Miranda (central bottom of part of outcrop shown in Figure 18; pencil is 140 mm long)**

The upper part of the Mount Goode Basalt contains areas of fine-grained metabasalt with generally less than 15%, but locally up to 30%, plagioclase phenocrysts. The plagioclase-phyric basalt is patchily developed but there is a remarkable example exposed at this stop, where phenocrysts are up to 200 mm across (Fig. 20). The abundance and size of the phenocrysts can vary greatly over a distance of less than 2 m. These phenocrysts probably crystallized in the magma chamber prior to eruption. Some are euhedral, but most are rounded due to partial resorption, which is thought to have occurred during magma ascent.

## Locality 10: Yakabindie Fault — AMG 51J $_{25}$88 $_{69}$449

### by S. F. Liu

At Locality 10, there is a well-exposed example of a typical shear zone, the Yakabindie Fault.

The Yakabindie Fault, just east of Yakabindie Homestead, trends at about 330°. It truncates the Kathleen Valley Gabbro and cuts the Mount Goode Basalt (Liu et al., 1996). In the Mount Goode Basalt the shear zone is about 50–100 m wide, and can be clearly seen on airphotos.

SW 34 26.08.97

**Figure 20. Metabasalt with abundant plagioclase phenocrysts (megacrysts) near the north shore of Lake Miranda**

Basaltic rocks in the shear zone contain a pronounced foliation (334°/84° NE) and a steep, northwest-plunging mineral lineation (64°→335°). In some outcrops the lineation is defined by elongate plagioclase aggregates after plagioclase phenocrysts. Basalt adjacent to the fault is relatively undeformed.

Sinistral movement on the Yakabindie Fault is indicated by a change in the trend of structures in the Kathleen Valley Gabbro from generally east-northeasterly to north-northeasterly in the vicinity of the Yakabindie and Highway Faults (Liu et al., 1996). This is consistent with structures at Lake Miranda (Locality 9), small-scale structures in the Highway Fault, and large-scale aeromagnetic trends (such as the asymmetry in the large, deformed monzogranite body east of the Perseverance Fault; Liu et al., 1997).

## Locality 11: Andalusite and cordierite porphyroblasts in quartzofeldspathic schist — AMG 51J 2599 69504

**by S. F. Liu**

A unit of interleaved amphibolite and peraluminous quartzofeldspathic schist outcrops just to the north of an easterly trending track, about 2.4 km north of Mount Goode. The unit is only about 100 m wide and trends north-northwest for about 700 m. Massive fine-grained tholeiitic basalt (Mount Goode Basalt) lies to the west of the schist, west of an interpreted fault (Liu et al., 1996). Contacts between the schist and basalt to the east and south are not exposed, but they may also be faulted.

The quartzofeldspathic schist contains relic bedding features and varying proportions of andalusite and/or (altered) cordierite porphyroblasts. The andalusite porphyroblasts are dull blue-green to white, measuring 5–10 mm in width and 10–20 mm in length (locally up to 40 mm in length; Fig. 21). They are randomly oriented in the plane of the schistosity. Some outcrops show a compositional layering marked by layers (10–50 mm thick) of abundant andalusite, which may reflect pelitic beds in the sedimentary protolith. Bedding trends at about 010°, whereas the regional

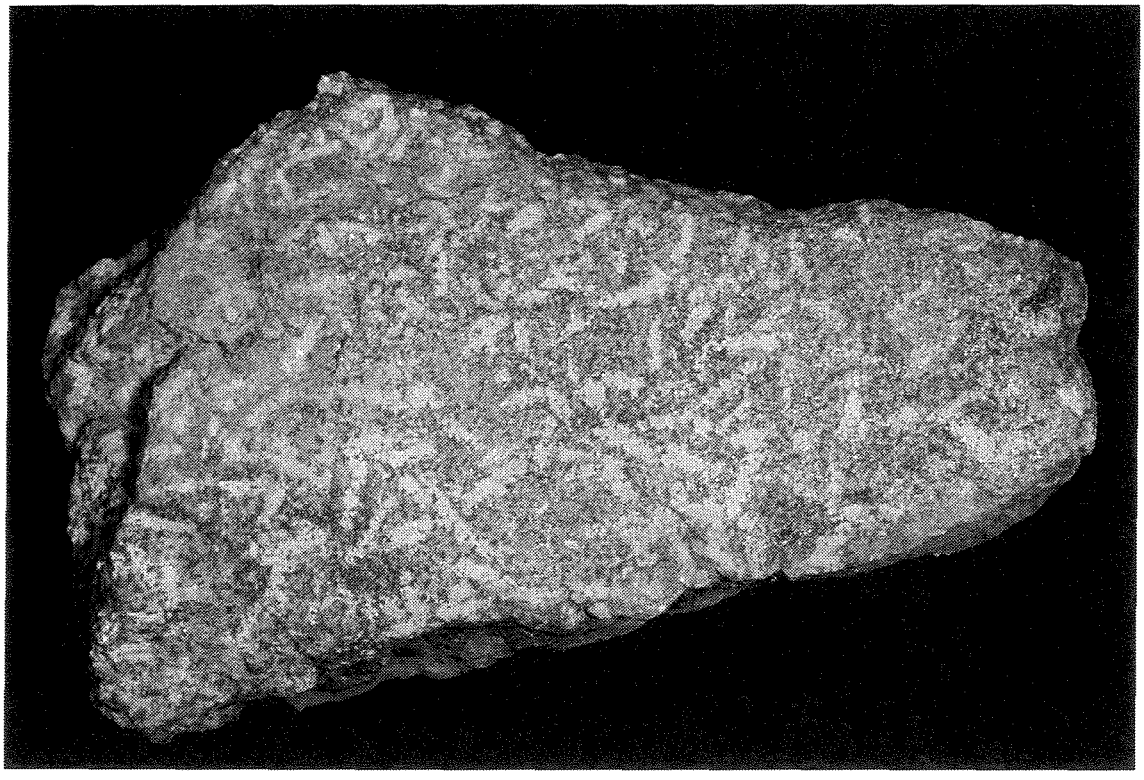

SW 36 27.08.97

**Figure 21. Randomly oriented andalusite porphyroblasts in peraluminous schist**

foliation trends at about 340°. Some parts of the outcrop contain brown discoid aggregates of very fine-grained alteration minerals after cordierite porphyroblasts. They lie in the plane of the foliation and are typically 10 to 20 mm in diameter, but may reach a maximum size of 30 mm. A flat-lying crenulation cleavage is developed locally.

## Locality 12: Felsic volcanic/volcaniclastic rock — Kathleen Valley — AMG 51J 2602 69534

### by S. F. Liu

Felsic volcanic and/or volcaniclastic rocks are abundant in the Agnew–Wiluna belt. However, they are usually deeply weathered and identification is difficult. A narrow, north-trending unit of massive felsic volcanic and/or volcaniclastic rocks is present about 1 km east of Kathleen (Liu et al., 1996). The unit lies between a fine-grained tholeiitic basalt unit to the west and a high-Mg basalt unit to the east.

The felsic unit contains massive crystal-rich volcanic sandstone, lapillistone, and minor conglomerate (Fig. 22). These rocks are probably primary pyroclastic deposits. Most clasts are angular to subangular and consist of porphyry or crystal-rich felsic volcanic rock. Clasts of fine-grained mafic schist and metasedimentary rocks are a minor component. The matrix is quartzofeldspathic, and in places the boundaries between the clasts and matrix are diffuse. The clasts are poorly sorted and range in size from a few mm to 100 mm across, but may be locally up to 400 mm in diameter. Some of the siltstone and mafic clasts have biotite-rich rims and pale haloes of fine-grained quartzofeldspathic material, suggesting a possible reaction between the clasts and a hot matrix at the time of deposition (Fig. 23).

Felsic tuff at Kathleen Valley (AMG 51J 2602 69533) has a characteristic blotchy appearance with pale-grey to white patches 10–100 mm across in a darker grey host. The pale patches consist of feldspar, quartz and amphibole with a grainsize of 1–2 mm and have margins that range from sharp to diffuse. The amphibole (probably hornblende) forms long prisms and makes up 5–10% of the volume. The finer grained grey material surrounding the pale patches contains biotite. This blotchy appearance may reflect small variations in fluid content of the original magma. In other outcrops in this area, the pale patches are more veinlike and, in some cases, associated with thin quartz veins.

Finer grained, more even-textured felsic rocks in this unit contain gradational layering on a scale of 100 mm on weathered surfaces.

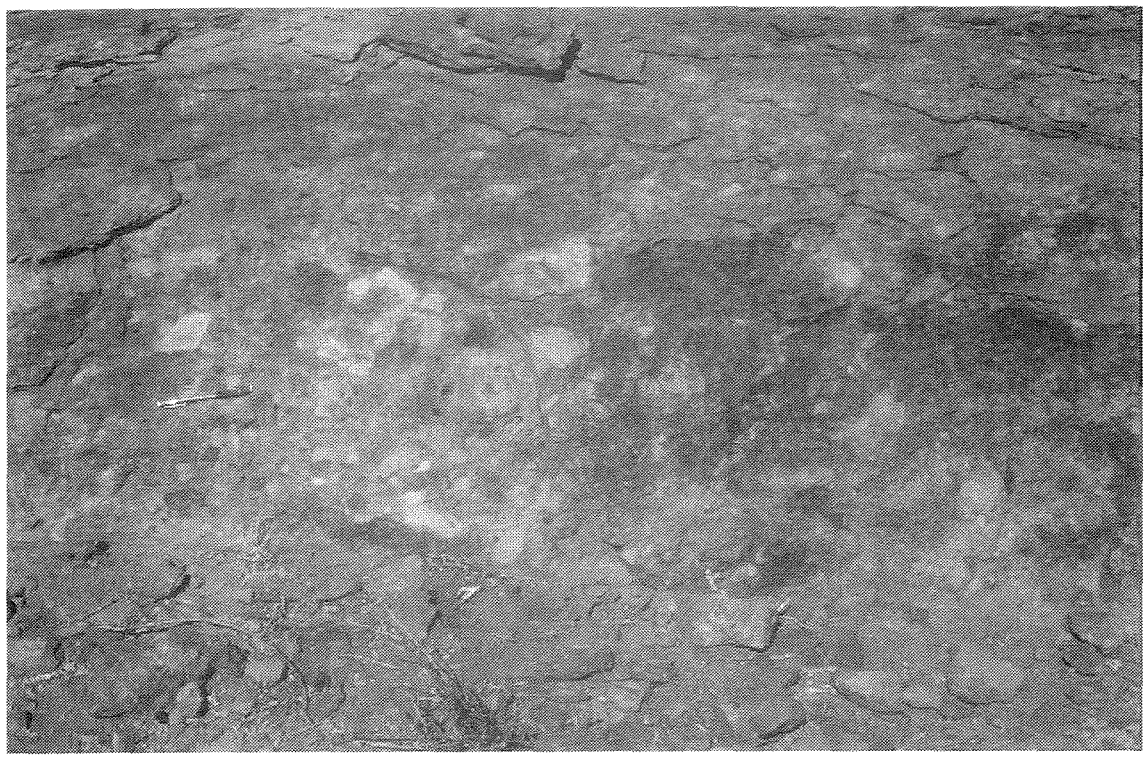

**Figure 22. Possible felsic lapilli tuff from 2 km southeast of Kathleen (pencil is 140 mm long)**

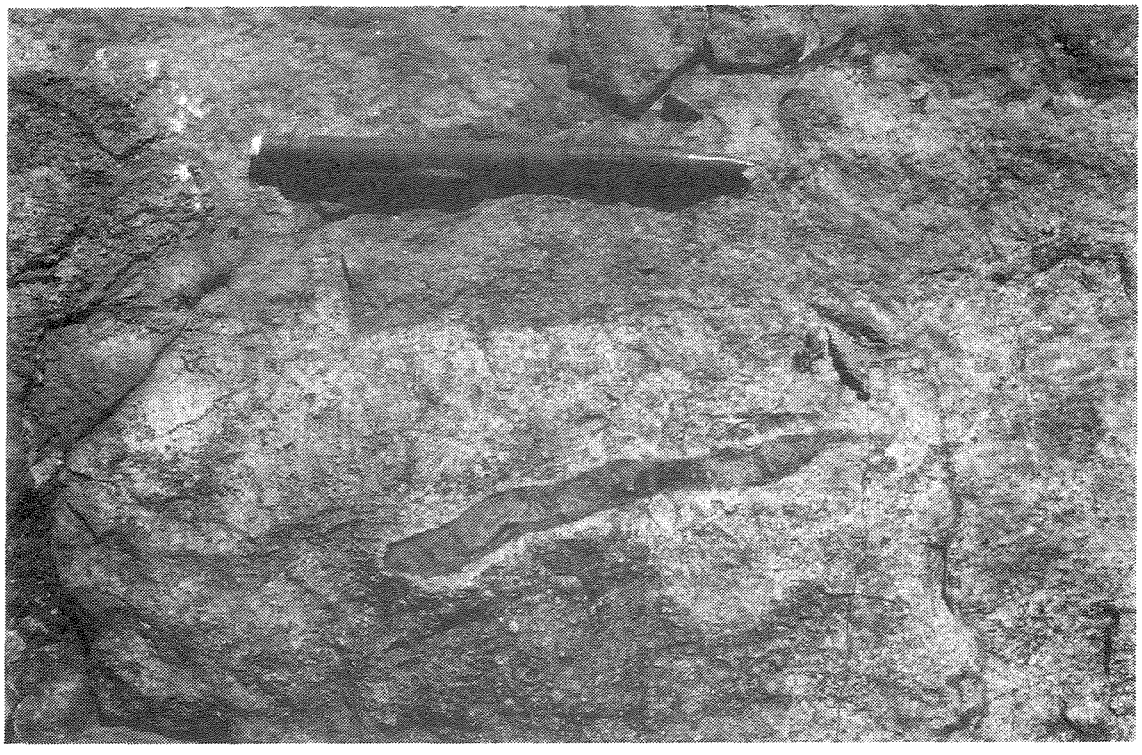

**Figure 23. Reaction rim around a metasiltstone clast in an outcrop of felsic tuff 2 km southeast of Kathleen (*pencil is 140 mm long*)**

## Locality 13: Jones Creek Conglomerate

### by S. F. Liu

The Jones Creek Conglomerate may be analogous to other Archaean conglomerates in similar settings, such as the Kurrawang Formation, the Penny Dam conglomerate, and the Yilgangi conglomerate in the southern part of the Eastern Goldfields Province (Swager et al., 1995; Swager, 1995), and to conglomerates in greenstone belts to the east, such as in the Duketon greenstone belt (Langford and Farrell, in prep.).

Marston and Travis (1976) described the variety of rock types in the Jones Creek area. These include granitoid metaconglomerate with granitoid clasts in an arkosic matrix; metaconglomerate with granitoid, felsic, and mafic clasts in a mafic matrix; mafic metaconglomerate; meta-arkose; and mafic and ultramafic metasedimentary schists. The meta-arkose is bedded, with low-angle cross-stratification, which indicates younging to the east. Near Jones Creek the conglomerate is deformed and has undergone lower amphibolite-facies metamorphism. There is no indication of a different metamorphic history from that of the surrounding greenstones (Marston and Travis, 1976).

Durney (1972) mapped the Jones Creek Conglomerate from near Six Mile Well to west of Agnew, a distance of more than 80 km (Fig. 2). He interpreted the conglomerate as a major unconformity in the Archaean Yilgarn Craton between a lower greenstone sequence in the west and an upper greenstone sequence in the east.

However, Marston and Travis (1976) noted that although the western contact between the Jones Creek Conglomerate and the underlying granitoids and greenstones is a deformed unconformity, the eastern contact between the conglomerate and the greenstones is so strongly deformed that its original nature cannot be determined. Moreover, Marston and Travis (1976) and Marston (1978) suggested that, rather than an unconformity between two greenstone sequences, the Jones Creek Conglomerate represents the youngest Archaean formation in the Agnew–Wiluna belt. The very immature nature of most of the clasts within the conglomerate indicates that they were locally derived. The Agnew–Wiluna belt east of the Jones Creek Conglomerate is structurally complex but generally youngs to the west (Naldrett and Turner, 1977). The Yakabindie sequence, to the west of the conglomerate, youngs to the southeast. Marston and Travis (1976) presented a model in which the conglomerate represents alluvial-fan deposits in a linear, partly fault-bounded basin with a granitoid–mafic source area to the west and a mafic–ultramafic source area to the east.

Nelson (1997) has obtained SHRIMP U–Pb ages of zircons from the arkosic matrix in the conglomerate and from the underlying monzogranite. The age of the monzogranite is 2685 ± 7 Ma. Several populations of zircons were identified in the conglomerate matrix, including zircons possibly derived from the monzogranite. A group of zircons with an age of 2632 ± 13 Ma provides a constraint on the maximum age of deposition of the arkose, suggesting that the conglomerate was deposited after approximately 2632 Ma. This, in turn, implies that there was a major episode of deformation and metamorphism after approximately 2632 Ma.

### Stop 13A: The unconformity at Jones Creek — AMG 51J 2589 6920

On the western side of Jones Creek, west of the Six Mile Well exploration camp, the Jones Creek Conglomerate occupies channel-like embayments in the underlying monzogranite (Durney, 1972). At the excursion locality, meta-arkose is draped over a protuberance of monzogranite in one of these embayments (Fig. 24). This locality was shown in Durney (1972, plate 9, fig. 2) and described by Marston and Travis (1976, fig. 5b). Cross-beds immediately to the east of the contact indicate younging to the east. The meta-arkose and the matrix of the metaconglomerate consist of quartz, plagioclase, microcline, biotite and muscovite. They have been markedly recrystallized and contain a fabric defined by preferred alignment of mica, quartz and feldspars (Marston and Travis, 1976; Nelson, 1997). Conglomerate near the base of the unit contains subangular to well-rounded boulders and cobbles of monzogranite very like that which outcrops immediately below the unconformity. Further east the metaconglomerate contains a greater range of clast types and includes intervals with an amphibolite matrix (Stop 13B).

### Stop 13B: Metaconglomerate with mafic matrix — AMG 51J 2596 6936

Mafic metaconglomerate and polymictic metaconglomerate with a mafic matrix have been identified in numerous outcrops between Mount Keith and Agnew (Durney, 1972; Marston and Travis, 1976; Liu et al., 1996; Jagodzinski and Stewart, in prep.). Mafic metaconglomerate has a restricted areal extent, but metaconglomerate with a mafic matrix and a diverse range of clast types is quite widespread, and increases in abundance towards the central part of the Jones Creek Conglomerate. Clast types include a variety of granitoids, metamorphosed felsic volcanic rocks, and less-abundant metasedimentary and mafic rocks (Marston and Travis, 1976). Marston and Travis (1976) interpret the diversity of clast types in the mafic-matrix metaconglomerate as an indication that it was deposited at some distance from the granitoid source area.

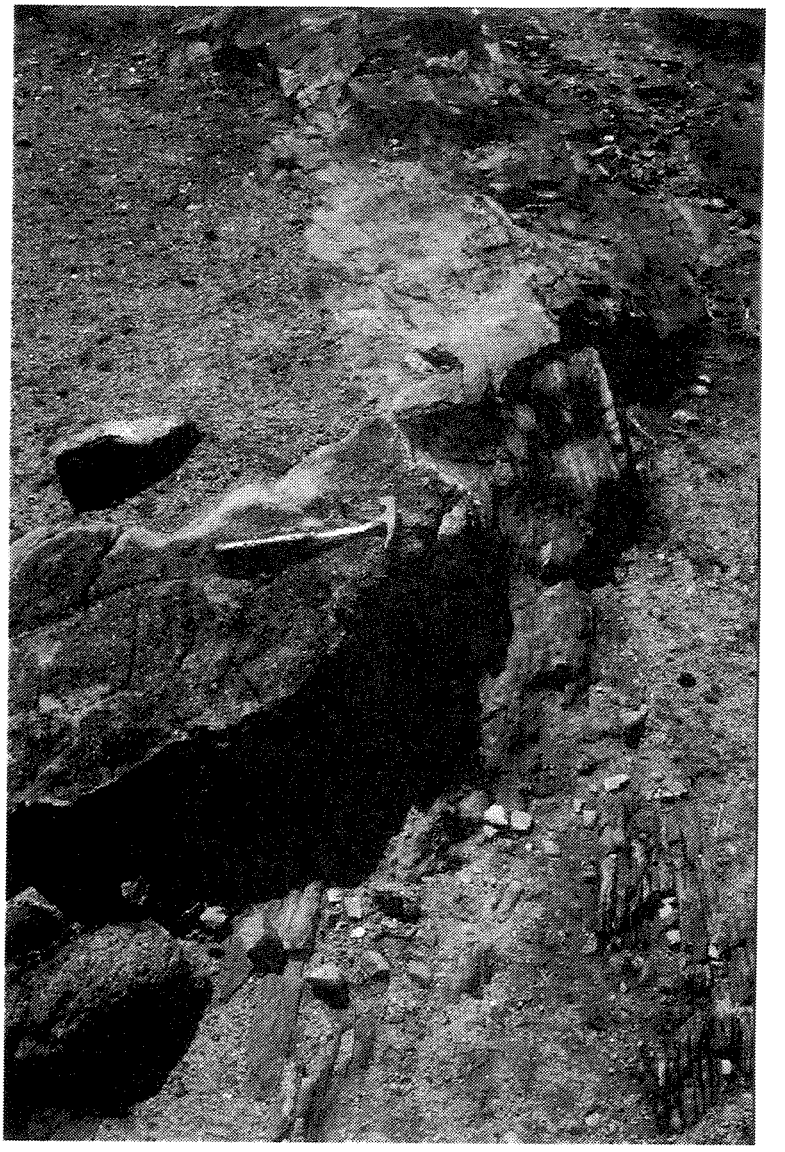

**Figure 24. Bedded arkosic sandstone of the Jones Creek Conglomerate draped over monzogranite**

At this stop an exposure in the side of a creek shows an example of mafic-matrix metaconglomerate with a range of clast types, including medium-grained granitoid, porphyritic granitoid, aplite and vein quartz. The matrix of the metaconglomerate typically contains hornblende, quartz, feldspar, biotite and clinozoisite (Marston and Travis, 1976). Thin layers of sandy quartzofeldspathic matrix have been boudinaged during strong compressional deformation. There is a well-developed foliation in the mafic matrix, similar in orientation to the regional foliation in the adjacent greenstones.

## Stop 13C: ?Hydraulic breccia — AMG 51J 2592 69563

An unusual outcrop of the Jones Creek Conglomerate (Fig. 25) has a number of characteristics consistent with the interpretation that at least some of this material is a hydraulic breccia.

The metaconglomerate at this stop is essentially monomictic, containing rounded, medium-grained granitoid clasts in a quartz–feldspar–biotite matrix. Features of this outcrop, consistent with the hydraulic breccia interpretation, are: (i) jigsaw-fit texture in some broken clasts, and (ii) planar fracturing in the western part of the outcrop.

Similar textures have been noted in gold-mineralized diamond drillcore at the Mossbecker mine, 2.2 km to the south (Liu et al., 1996). The drillcore consists of mafic-matrix metaconglomerate dominated by felsic porphyry clasts, but also including clasts of granitoid, mafic and metasedimentary rock.

## Stop 13D: Polymictic metaconglomerate — AMG 51J 2590 69574

At stop 13D, metamorphosed polymictic metaconglomerate of the Jones Creek Conglomerate contains a range of subangular to well-rounded cobbles and boulders of granitoid in a

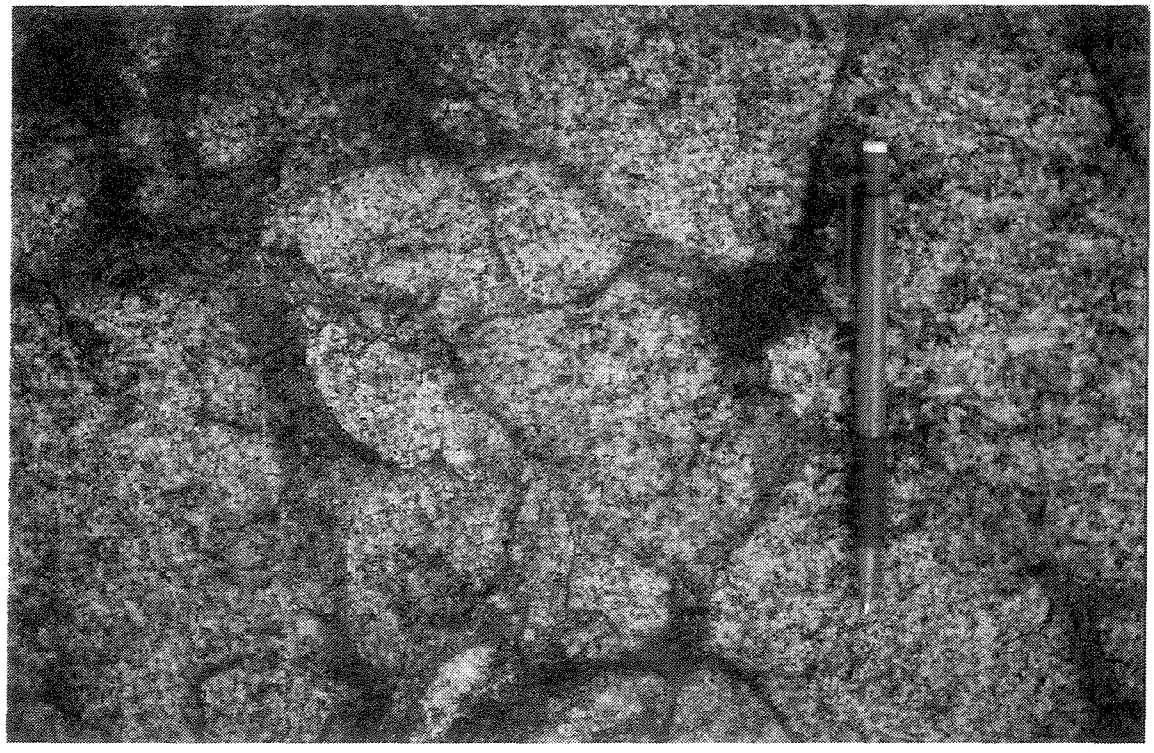

**Figure 25. Jigsaw-fit of clasts in possible hydraulic breccia (pencil is 140 mm long)**

recrystallized arkosic matrix. The granitoid clasts include a variety of compositions and textures. Rare mafic and pegmatite clasts are also present. Some clasts contain quartz veins and there are quartz veins that cut the entire outcrop. There is no evidence of bedding in this outcrop.

## Locality 14: Mount Keith nickel mine

### by M. Fletcher and S. Hopf

The Mount Keith Nickel Operation is located about 80 km south of Wiluna on SIR SAMUEL (1:250 000; Bunting and Williams, 1979). WMC Resources acquired an interest in the project in 1991 by a takeover of Mount Keith ACM and then gained 100% ownership in 1993.

Nickel mineralization was first identified at Mount Keith in 1968 by the pastoralist, Mr Jim Jones. Mr Jones drilled a hole into ultramafic outcrop about 1 km south of the current orebody using a water-boring cable-tool rig. Sulfides were noted in the panned drill samples, which were assayed and shown to be anomalous in nickel. After viewing these results, Metals Exploration acquired the lease holding and drilled the discovery diamond drillhole, MKD 5, in December 1969.

Ore reserves for the MKD5 deposit (named after the discovery hole) were 173 Mt at 0.61% Ni for a mine life of about 20 years at 30 June 1996. The operation is currently producing about 10.5 Mt per annum of ore for 42 000 t Ni concentrate. The orebody is mined by opencut methods, with a final pit design measuring 2.5 km in length by 1.5 km in width and 480 m deep (cut-back stage G).

### Regional geology

The Mount Keith deposit is located in the centre of the Agnew–Wiluna part of the Norseman–Wiluna greenstone belt (Fig. 26). In the Mount Keith area, the greenstone belt comprises komatiite, basalt (with high MgO in some places), gabbro, and felsic to intermediate volcanic and volcanogenic sedimentary rocks, plus minor chert and carbonaceous shale. Granitoids bound these rocks to the east and west. The metamorphic grade ranges from prehnite–pumpellyite facies at Wiluna, to upper amphibolite facies in the Leinster area. The sequence at Mount Keith has undergone mid-greenschist facies metamorphism. Northwest faulting (associated with the Keith–Kilkenny Lineament) is the major structural feature, and regionally less-significant structures cut across the belt at various trends.

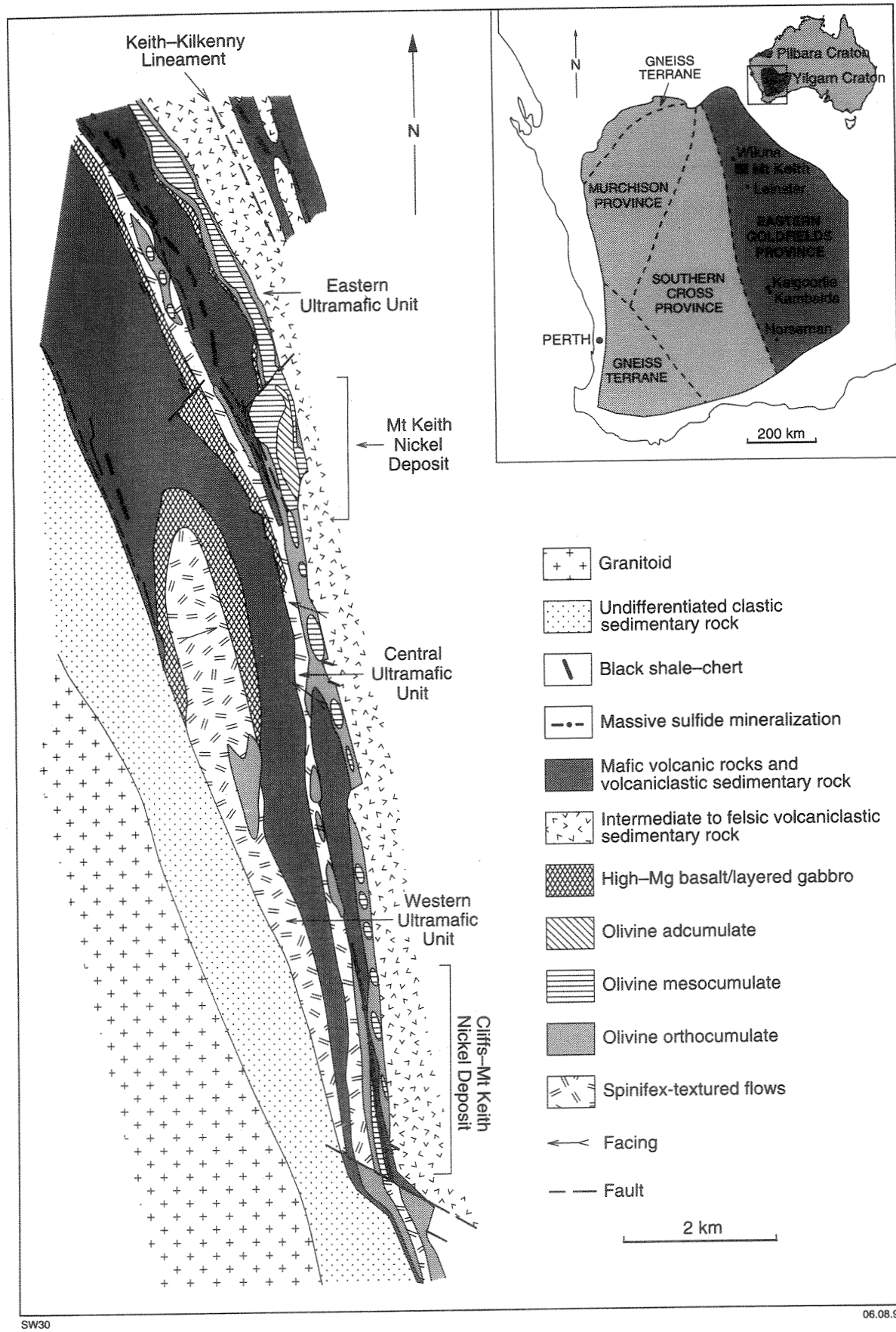


**Figure 26. Simplified geological map of part of the Agnew–Wiluna greenstone belt showing the location of the Mount Keith nickel deposit (after Dowling and Hill, 1990). The inset shows the location of Mount Keith in the Eastern Goldfields Province**

Komatiite flow units can be traced for over 100 km from Perseverance to Honeymoon Well. At least three discrete flow units, named the Eastern, Central and Western Ultramafic units (EUM, CUM, and WUM, respectively; Fig. 26) have been identified between the prospects at Six Mile Well (Yakabindie) and Kingston (Dowling and Hill, 1990). The units are generally west-facing with olivine spinifex and cumulate textures indicating the younging direction of the flows. Orthocumulate textures characterize the komatiite units, but adcumulate–mesocumulate layered textures also occur in thickened zones (channel positions).

Two models for nickel mineralization in the Agnew–Wiluna Belt have been described by Hill and Gole (1990):

(i) *Class I:* Massive-sulfide mineralization at the base of relatively thin, ultramafic, komatiitic lava flows. Orebody widths of less than 20 m and nickel grades between 2 and 15 wt% characterize this type. Examples are the Cliffs–Charterhall (10 km south of Mount Keith) and Perseverance deposits.

(ii) *Class II:* Disseminated sulfide mineralization within thickened zones (between 100 m and 300 m width) of the komatiite flow, commonly with a dunitic composition. These deposits are generally low in grade (about 0.6 wt% Ni) and large in tonnage (>100 Mt). Examples include Mount Keith, Honeymoon Well and Yakabindie.

## Local geology

The MKD5 Ultramafic Unit (EUM of Dowling and Hill, 1990) hosts the Mount Keith deposit (Figs 27 and 28) and has a maximum thickness of about 600 m. The unit can be divided into three lithologically distinct zones (Fig. 27): (i) a basal olivine orthocumulate; (ii) a central zone containing an unmineralized, coarse-grained olivine adcumulate, which grades upwards into a layered olivine–sulfide adcumulate/mesocumulate (Mount Keith orebody); and (iii) an upper orthocumulate containing zones of gabbroic ultramafic differentiate. Unmineralized porphyritic olivine rocks occur in three stratiform layers from 0.5 to 1.5 m thick, in the upper part of the olivine adcumulate and the basal part of the olivine–sulfide mesocumulate (Seymon, 1996).

The base of the hangingwall sequence contains a pyrite-rich sedimentary rock/chert layer at the MKD 5 Ultramafic Unit contact. This has a maximum thickness of 10 m in the north, but is absent to the south. It is generally overlain by a thin carbonaceous shale layer (up to 1 m thick), which is overlain by a sequence of intermediate volcaniclastic rocks (up to 50 m thick) and a sequence of basalt and dolerite (up to 50 m thick). The volcaniclastic rocks contain interbedded

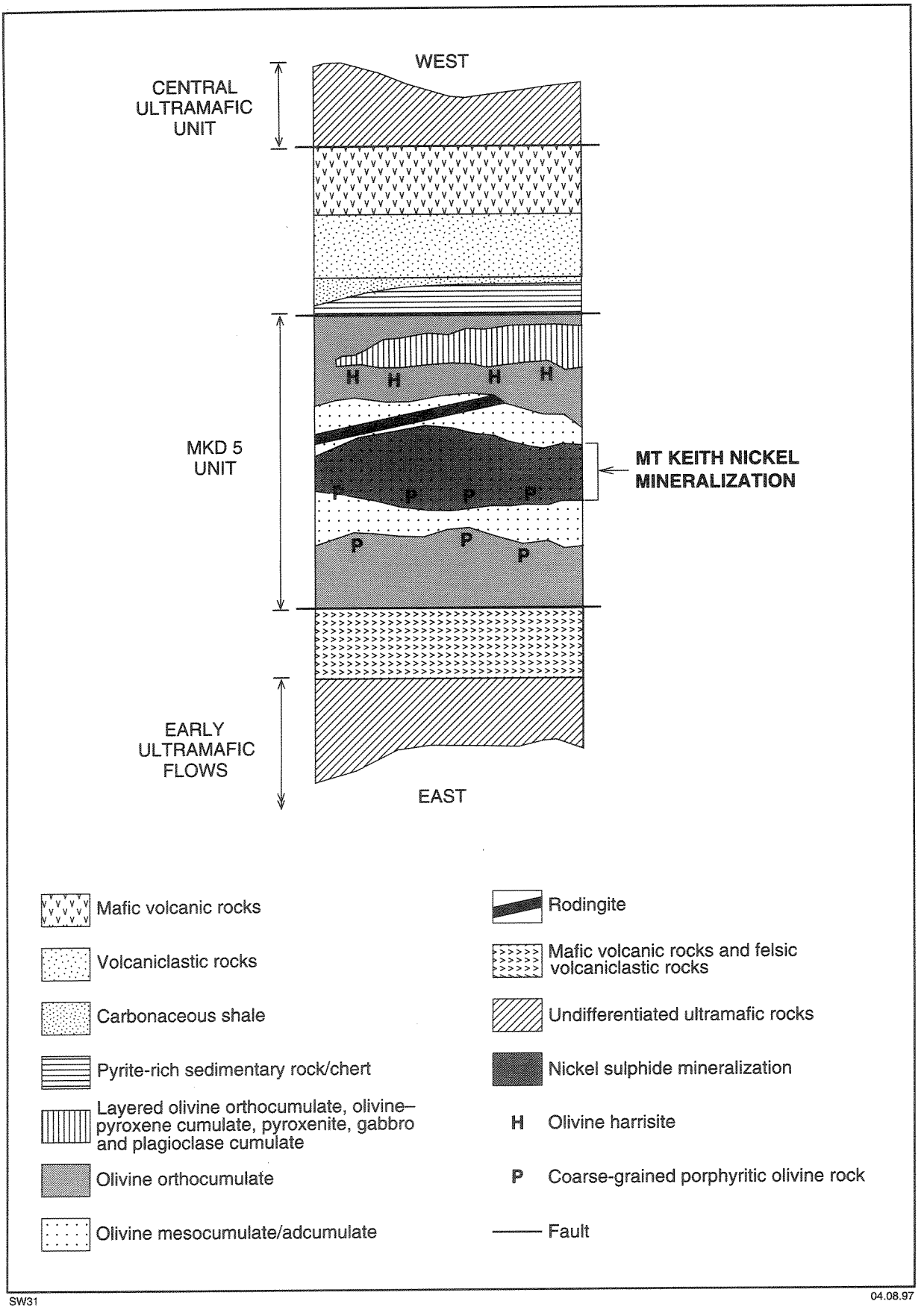


**Figure 27. Schematic stratigraphic column for the greenstone sequence in the Mount Keith area**

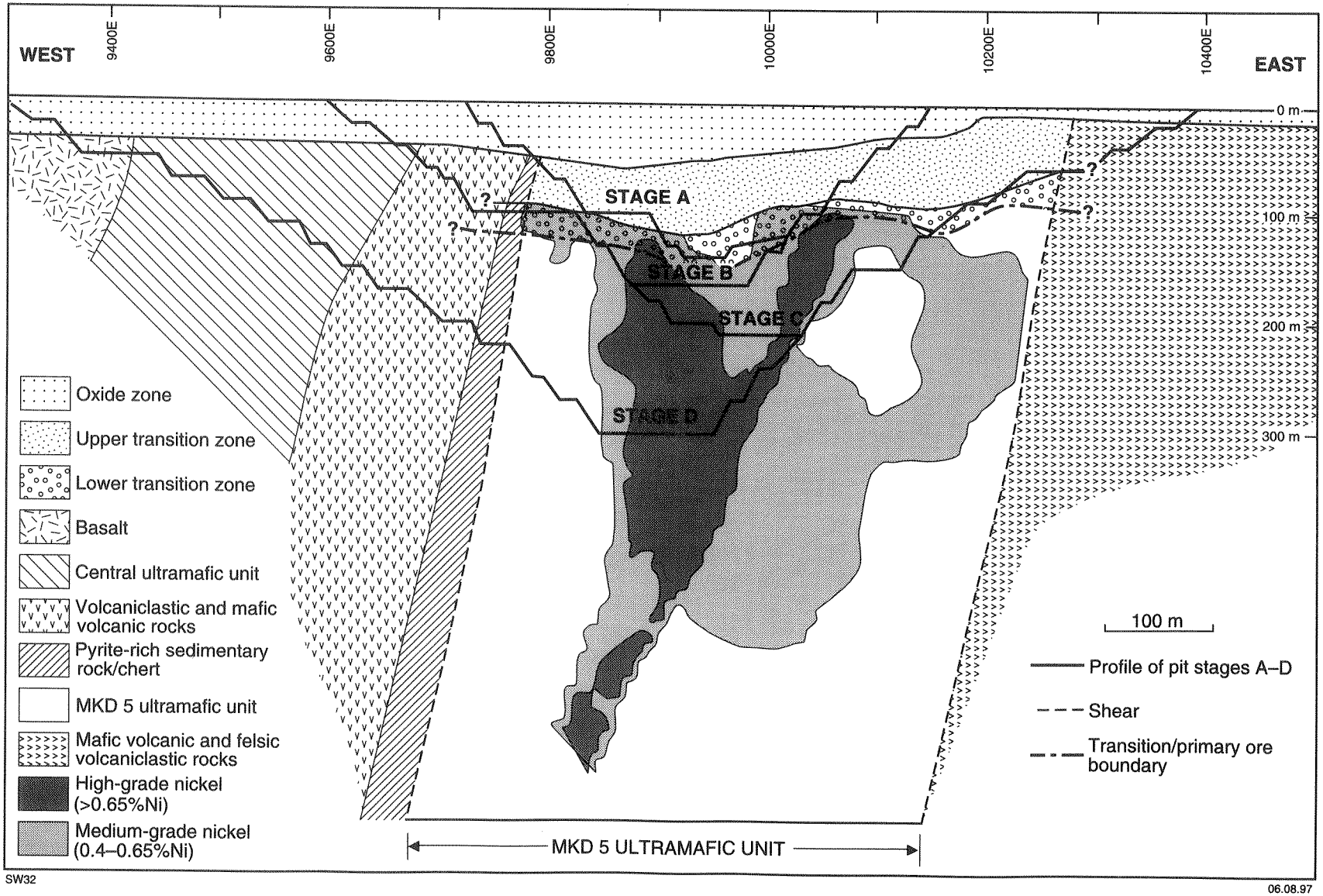


**Figure 28. Simplified geological cross section of the Mount Keith deposit showing the distribution of the Oxide, and the Upper and Lower Transition Zones. The position of medium- and high-grade nickel mineralization in the MKD 5 Unit is also shown. Stages A to D refer to the pit designs (current mining is in Stage D pit)**

thin layers of carbonaceous shale, and in the upper part are intercalated with the overlying mafic rocks. The sequence of mafic rocks is overlain by the third and uppermost komatiitic unit (CUM). The footwall sequence consists of volcaniclastic sedimentary rocks and mafic volcanic rocks.

Both the hangingwall and footwall contacts of the MKD 5 Ultramafic Unit (EUM) are extensively sheared and carbonated, whereas the central parts are only weakly deformed. Carbonated splay faults crosscut and displace the ultramafic unit and the orebody. One southeasterly trending splay offsets the southern part of the orebody by about 90 m to the east (Mill, J., 1997, pers. comm.). Intense talc–carbonate alteration, commonly brecciated and fractured by later movement, is often associated with these structures.

Primary igneous textures are commonly well preserved, although pervasive serpentinization accompanied greenschist-facies metamorphism of the MKD 5 Ultramafic Unit. Primary olivine crystals have been pseudomorphed by lizardite, and the intercumulus areas typically contain brucite, stichtite (a chromium-bearing hydroxycarbonate after igneous chromite), and pyroaurite.

Carbonate alteration of the ultramafic rocks occurs in, or adjacent to, strongly fractured or sheared zones and has resulted in the overprinting of the serpentinite assemblages. Three main types of alteration have been recognized, though a gradation exists from one alteration type to the other. Intense carbonate(–talc) alteration occurs along the margins of the MKD 5 Unit and along faults and fractures. Adjacent to these zones the carbonate alteration is weaker and the rocks contain lizardite and antigorite with smaller amounts of carbonate (proximal carbonate alteration). Farther away from the fracture zones, the serpentinite contains abundant hydroxycarbonates and trace amounts of carbonate (distal carbonate alteration).

## Mineralization

Nickel mineralization at Mount Keith is dominantly hosted by olivine adcumulate and mesocumulate in the central part of the MKD 5 Ultramafic Unit. Pentlandite is the main nickel sulfide mineral. Millerite is much less abundant, and is typically restricted to carbonated zones. Accessory minerals include gersdorffite, niccolite, cobaltite and maucherite. The orebody is broadly zoned from a pyrrhotite-dominated hangingwall, through a pentlandite–pyrrhotite zone, to a pentlandite-dominated lower zone. In parallel with the ore zoning, the nickel tenor of the ore (Ni content of the sulfide assemblage) typically increases towards the footwall contact.

Primary magmatic nickel sulfides occur mainly in lobate aggregates in the interstices between former olivine grains. The aggregates are typically 1–2 mm in diameter but may attain a maximum

size of 8 mm. They consist of a magnetite rim and a core with geometric intergrowths of magnetite and coarse-grained pentlandite(–pyrrhotite). Carbonation has resulted in the partial replacement of sulfide aggregates by gangue minerals (such as carbonate and serpentine minerals) and the partial or complete replacement of pentlandite by millerite. Fine-grained nickel sulfides are also present within former olivine grains. In intensely carbonated rocks the primary sulfide aggregates are almost completely replaced by gangue, and the sulfides are finely disseminated and commonly occur in lamellar intergrowths with gangue minerals.

## Acknowledgements

The GSWA and AGSO would like to thank the staff and management at Great Central Mines Bronzewing Gold Operations and at WMC Resources Mount Keith Operation for their assistance in the preparation of this excursion guide and the organization of the excursion.

# References


BUNTING, J. A., and WILLIAMS, S. J., 1979, Sir Samuel, W.A. Sheet SG 51 — 13: Western Australia Geological Survey, 1:250 000 Geological Series Explanatory Notes, 40p.

COMPSTON, W., WILLIAMS, I. S., CAMPBELL, I. H., and GRESHAM, J. J., 1986, Zircon xenocrysts from the Kambalda volcanics: age constraints and direct evidence for older continental crust below the Kambalda–Norseman greenstones: Earth and Planetary Science Letters, v. 76, p. 299–301.

DOWLING, S. E., and HILL, R. E. T., 1990, Rivers of fire: the physical volcanology of komatiites of the Mount Keith region, Norseman–Wiluna belt, Western Australia: CSIRO Exploration Geoscience Restricted Report 103R, 170p.

DURNEY, D. W., 1972, A major unconformity in the Archaean, Jones Creek, Western Australia: Journal of the Geological Society of Australia, v. 19, p. 251–259.

ESHUYS, E., HERBISON, I., PHILLIPS, N., and WRIGHT, J., 1995, Discovery of Bronzewing gold mine, *in* New generation gold mines: case histories of discovery: Australian Mineral Foundation, Adelaide, p. 2.1–2.15.

ESHUYS, E., and LEWIS, C. R., 1995, New approaches to gold exploration, *in* Proceedings of the Outlook 95 Conference: Australian Bureau of Agriculture and Resource Economics, Canberra, p. 336–340.

FARRELL, T. R., 1995, Structural geology of the Duketon area, northeastern Goldfields: Western Australia Geological Survey, Annual Review 1994–95, p. 89–93.

GILES, C. W., 1980, A comparative study of Archaean and Proterozoic felsic volcanic associations in southern Australia: University of Adelaide, PhD thesis (unpublished).

GILES, C. W., 1982, The geology and geochemistry of the Archaean Spring Well felsic volcanic complex, Western Australia: Journal of the Geological Society of Australia, v. 29, p. 205–220.

GRIFFIN, T. J., 1990, Southern Cross Province, *in* Geology and mineral resources of Western Australia: Western Australia Geological Survey, Memoir 3, p. 60–77.

HALLBERG, J. A., 1985, Geology and mineral deposits of the Leonora–Laverton area, northeastern Yilgarn Block, Western Australia: Perth, Western Australia, Hesperian Press, 140p.

HALLBERG, J. A., and GILES, C. W., 1986, Archaean felsic volcanism in the northeastern Yilgarn Block, Western Australia: Australian Journal of Earth Sciences, v. 33, p. 413–427.

HAMMOND, R. L., and NISBET, B. W., 1992, Towards a structural and tectonic framework for the central Norseman–Wiluna greenstone belt, Western Australia, *in* The Archaean: terrains, processes and metallogeny *edited by* J. E. GLOVER and S. E. HO: University of Western Australia, Geology Department (Key Centre) and University Extension, Publication 22, p. 39–49.

HILL, R. E. T., BARNES, S. J., GOLE, M. J., and DOWLING, S. J., 1995, The volcanology of komatiites as deduced from field relationships in the Norseman–Wiluna greenstone belt, Western Australia: Lithos, v. 34, p. 159–188.

HILL, R. E. T., and GOLE, M. J., 1990, Nickel sulphide deposits of the Yilgarn Craton, *in* Geology of the Mineral Deposits of Australia and Papua New Guinea, v. 1 *edited by* F. E. HUGHES: The Australasian Institute of Mining and Metallurgy, Melbourne, p. 557–559.

JAGODZINSKI, E. A., and STEWART, A. J., in prep., Mount Keith, W.A. Sheet 3043: Australian Geological Survey Organisation, 1:100 000 Geological Series.

LANGFORD, R. L., and FARRELL T. R., in prep., Geology of the Duketon 1:100 000 sheet: Western Australian Geological Survey, 1:100 000 Geological Series Explanatory Notes.

LIU, S. F., GRIFFIN, T. J., WYCHE, S., and WESTAWAY, J. M., 1996, Sir Samuel, W.A. Sheet 3042: Western Australia Geological Survey, 1:100 000 Geological Series.

LIU, S. F., GRIFFIN T. J., WYCHE, S., FERGURSON, K. M., WESTAWAY, J. M., in prep., The geology of the Sir Samuel 1:100 000 sheet: Western Australia Geological Survey, 1:100 000 Geological Series Explanatory Notes.

MARSTON, R. J., 1978, The geochemistry of Archaean clastic metasediments in the relation to crustal evolution, northeastern Yilgarn Block, Western Australia: Precambrian Research, v. 6, p. 157–175.

MARSTON, R. J., and TRAVIS, G. A., 1976, Stratigraphic implications of heterogeneous deformation in the Jones Creek Conglomerate (Archaean), Kathleen Valley, Western Australia: Journal of the Geological Society of Australia, v. 23, p. 141–156.

NALDRETT, A. J., and TURNER, A. R., 1977, The geology and petrogenesis of a greenstone belt and related nickel sulfide mineralization at Yakabindie, Western Australia: Precambrian Research, v. 5, p. 43–103.

MYERS, J. S., 1995, The generation and assembly of an Archaean supercontinent: evidence from the Yilgarn craton, Western Australia, *in* Early Precambrian Processes, *edited by* M. P. COWARD and A. C. RIES: Geological Society Special Publication No. 95, p. 143–154.

NELSON, D. R., 1995, Compilation of SHRIMP U–Pb zircon geochronology data, 1994: Western Australia Geological Survey, Record 1995/3, 244p.

NELSON, D. R., 1996, Compilation of SHRIMP U–Pb zircon geochronology data, 1995: Western Australia Geological Survey, Record 1996/5, 168p.

NELSON, D. R., 1997, Compilation of SHRIMP U–Pb zircon geochronology data, 1996: Western Australia Geological Survey, Record 1997/2, 189p.

NELSON, D. R., in prep., Compilation of SHRIMP U–Pb zircon geochronology data, 1997: Western Australia Geological Survey, Record.

PASSCHIER, C. W., 1994, Structural geology across a proposed Archaean terrane boundary in the eastern Yilgarn Craton, Western Australia: Precambrian Research, v. 68, p. 43–64.

PHILLIPS, G. N., ESHUYS, E., and HELLSTEN, K., 1996, Integrated exploration techniques for Archaean gold, Western Australia, *in* Diversity: the key to prosperity: Annual Conference, Australasian Institute of Mining and Metallurgy, Perth, 1996, Proceedings, p. 289–293.

PHILLIPS, G. N., VEARNCOMBE, J. R., BLUCHER, I., and RAK, D., in press, Bronzewing Gold Deposit, *in* Australasian Institute of Mining and Metallurgy, Monograph 22.

PLATT, J. P., ALLCHURCH, P. D., and RUTLAND, R. W. R., 1978, Archaean tectonics in the Agnew supracrustal belt, Western Australia: Precambrian Research, v. 7, p. 3–30.

SEYMON, A. R., 1996, Petrology and geochemistry of porphyritic olivine-rich rocks, Mount Keith W.A.: Monash University, Melbourne, Honours thesis (unpublished).

SWAGER, C. P., 1995, Geology of the greenstone terranes in the Kurnalpi–Edjudina region, southeastern Yilgarn Craton: Western Australia Geological Survey, Report 47, 31p.

SWAGER, C. P., 1997, Tectono-stratigraphy of late Archaean greenstone terranes in the Eastern Goldfields, Western Australia: Precambrian Research, v. 83, p. 11–42.

SWAGER, C. P., GRIFFIN, T. J., WITT, W. K., WYCHE, S., AHMAT, A. L., HUNTER, W. M., and McGOLDRICK, P. J., 1995, Geology of the Archaean Kalgoorlie Terrane — an explanatory note (reprint of Record 1990/12): Western Australia Geological Survey, Report 48, 26p.

SWAGER, C. P., GOLEBY, B. R., DRUMMOND, B. J., RATTENBURY, M. S., and WILLIAMS, P. R., 1997, Crustal structure of granite–greenstone terranes of the Eastern Goldfields, Yilgarn Craton, as revealed by seismic reflection profiling: Precambrian Research, v. 83, p. 43–56.

SWAGER, C. P., and NELSON, D. R., 1997, Extensional emplacement of a high-grade granite gneiss complex into low-grade greenstones, Eastern Goldfields, Yilgarn Craton: Precambrian Research, v. 83, p. 203–219.

WANG, Q., SCHIOTTE, L., and CAMPBELL, I. H., 1996, Geochronological constraints on the age of komatiites an nickel mineralisation in the Lake Johnston Greenstone Belt, Yilgarn Craton, Western Australia: Australian Journal of Earth Sciences, v. 44, p. 381–385.

WESTAWAY, J. M., and WYCHE, S., in prep., Geology of the Darlot 1:100 000 sheet: Western Australia Geological Survey, 1:100 000 Geological Series Explanatory Notes.

WILLIAMS, P. R., and WHITAKER, A. J., 1993, Gneiss domes and extensional deformation in the highly mineralised Archaean Eastern Goldfields Province, Western Australia: Ore Geology Reviews, v. 8, p. 141–162.

WITT, W. K., MORRIS, P. A., WYCHE, S., and NELSON, D. R., 1996, The Gindalbie Terrane as a target for VMS-style mineralization in the Eastern Goldfields Province of the Yilgarn Craton: Western Australia Geological Survey, Annual Review 1995–96, p. 41–47.

WYCHE, S., and WESTAWAY, J. M., 1995, Geology of the southern part of the Yandal greenstone belt, Eastern Goldfields: Western Australia Geological Survey, Annual Review 1994–95, p. 94–97.

WYCHE, S., and WESTAWAY, J. M., 1996, Darlot, W.A. Sheet 3142: Western Australia Geological Survey, 1:100 000 Geological Series.